



Review Paper

A review on the structure-performance relationship of the catalysts during propane dehydrogenation reaction

Bohan Feng, Yue-Chang Wei^{**}, Wei-Yu Song, Chun-Ming Xu^{*}

State Key Laboratory of Heavy Oil Processing, College of Science, China University of Petroleum, Beijing, 102249, People's Republic of China

ARTICLE INFO

Article history:

Received 10 February 2021

Accepted 29 March 2021

Available online 12 October 2021

Edited by Xiu-Qiu Peng

Keywords:

Dehydrogenation of propane

Metal catalysts

Oxide catalysts

Structure-performance relationship

Active site

Reaction mechanism

ABSTRACT

Dehydrogenation of propane (PDH) technology is one of the most promising on-purpose technologies to solve supply-demand unbalance of propylene. The industrial catalysts for PDH, such as Pt- and Cr-based catalysts, still have their own limitation in expensive price and security issues. Thus, a deep understanding into the structure-performance relationship of the catalysts during PDH reaction is necessary to achieve innovation in advanced high-efficient catalysts. In this review, we focused on discussion of structure-performance relationship of catalysts in PDH. Based on analysis of reaction mechanism and nature of active sites, we detailed interaction mechanism between structure of active sites and catalytic performance in metal catalysts and oxide catalysts. The relationship between coke deposition, co-feeding gas, catalytic activity and nanostructure of the catalysts are also highlighted. With these discussions on the relationship between structure and performances, we try to provide the insights into microstructure of active sites in PDH and the rational guidance for future design and development of PDH catalysts.

© 2022 The Authors. Publishing services by Elsevier B.V. on behalf of KeAi Communications Co. Ltd. This is an open access article under the CC BY-NC-ND license (<http://creativecommons.org/licenses/by-nc-nd/4.0/>).

1. Introduction

Propylene is one of most important petrochemical products, as it could build huge variety of chemical commodities. In traditional petrochemical technology network, cracking technology undertake most supply of propylene. Nowadays, more than three-fourths propylene is produced as a by-product by naphtha steam cracking and fluid catalytic cracking (FCC) (Bhasin et al., 2001; Hu et al., 2019; James et al., 2016; Nawaz, 2015; Wang et al., 2020; Al-Douri et al., 2017). However, the growth requirement of propylene cannot be satisfied. Facing challenges from supply and demand side, it is urgent to improve novel propylene generation technology. In recent years, a lot of attempts have been adopted to give traditionally cracking technology more flexibility and increase yield of propylene (Alabdullah et al., 2020). Coupling catalytic and thermal cracking process has been got attention, which deepen the cracking degree of reactant and widen feeding to wide-range oils. A novel cracking technology called DCC was developed by Sinopec Research Institute of Petroleum Processing. Base on FCC technology,

this technology further takes higher temperature and partial pressure of steam, which deepen cracking degree and thus produce more propylene (Akah and Al-Ghrami, 2015). However, the selectivity of propylene in these technologies is still poor and oil-feeding would cause serious energy-consumption (Blay et al., 2017). Some novel technologies called on-purpose propylene production technology has been attractive alternatives to traditional cracking process, such as oxidative coupling of methane, methanol to propylene, Fischer-Tropsch synthesis and direct dehydrogenation of propane (PDH). Compared with the traditional process, they have highly selectivity and don't need oil-feeding. (Hu et al., 2019). Recently, PDH due to cheap and widely available raw material (propane) receives much attention, this transformation from gas fuel (propane) to chemical product (propylene) also indicated huge economic profits. Thus, PDH is widely considered to the most promising propylene production technology in the future.

For improving industrial sufficiency of PDH, developing eco-friendly, cheap and active catalysts play the core role. At present, Pt and Cr-based catalysts are successfully industrialized, and various kinds of (Ga, V, Zn, Zr, Ni, Co, Fe, Al, Sn, Mo and other noble metals) the catalysts have been studied and reported widely (Hu et al., 2019; Nawaz, 2015; Sattler et al., 2014). In order to provide a scientific understanding on these numerous catalysts, researches had made a lot of excellent reviews. Sattler et al., 2014 classified

* Corresponding author.

** Corresponding author.

E-mail addresses: weiy@cup.edu.cn (Y.-C. Wei), xcm@cup.edu.cn (C.-M. Xu).

common PDH catalysts by element and make a very detailed review on their reaction mechanism, promoter and support. [Hu et al., 2019](#) further widened types of catalyst and classified them into three categories: metal, metal oxide and carbon catalysts by an intuition of overall structure of materials. [Chen et al. \(2020\)](#) subdivided the existing metal and oxide catalysts based on the active site structure. However, the structure-performance relationship is rarely summarized and explained in basic principles of chemistry. For the oxide catalysts, most reviews are classified by elements ([Hu et al., 2019](#); [Nawaz, 2015](#); [Sattler et al., 2014](#)). In addition, the role of adsorbed gas and coke product on activity is also lacked summary. Therefore, the structure-performance relationship in propane dehydrogenation still needs to be outlined systematically.

In this review, we summarize theoretical and experimental researches achievement of catalysts in recent years. Reaction mechanism and nature of active sites are discussed in detail assisted by researches on well-defined model catalysts and density functional theory (DFT) calculations. Furthermore, we outline the effect of supports and promoter on structural and electronic properties of catalysts as well as their effect on catalytic performance. Coke formation, as the main culprit causing deactivation, its deposition mechanism and structure-activity relationship is highlighted. In the end, the influence of adsorption of co-feeding gas is introduced to emphasize importance of process intensification. We hope this paper would contribute rationally design and optimization PDH catalyst in the future.

2. Overview of PDH reaction

For understanding PDH processes intuitively, [Fig. 1](#) displays a simplified process of main and side reactions in PDH reaction. Formation of equimolar propylene from propane is the main reaction of PDH. Side reactions include cracking, hydrogenolysis and coke deposition. Some other side reaction such as oligomerization, cyclization also happened but occupy a small part. Cracking

includes a group reaction of cleavage hydrocarbons to two smaller alkene or alkane. Their pathway in PDH includes two mechanisms: thermal cracking and catalytic cracking. Coke deposition refers to formation various carbon-rich hydrocarbons or macromolecule solid carbon though deep dehydrogenation. Due to its gas-solid two-phase reaction, thus it is not limited by reaction equilibrium in PDH. Both catalytic cracking and coke deposition are directly catalyzed through active sites or Lewis/Bronsted acidic sites. Specially, hydrogenolysis reaction initiate on the surface of metal, in which alkane would be converted into two smaller alkanes assisted by hydrogen ([Sattler et al., 2014](#)).

In the process of catalytic PDH, hydrogen atoms in propane would play a protecting role and prevent activation of C–C bonds. DFT calculations also proved breaking the C–C bond of alkane when the C–H bond is abundant are difficult, fracture energy of C–C bonds and C–H bonds would be lower with taking away hydrogen atoms([Yang et al. 2010, 2012](#); [Huš et al., 2020](#)). Therefore, propylene is widely thought as the key intermediates of side product of side reaction rather than propane, and it has a series reaction like relationship between side reaction and main reaction. ([Yang et al., 2010](#); [Nykänen and Honkala, 2011](#); [Valcárcel et al., 2002](#); [Yang et al., 2010](#)). The barriers of propylene desorption and dehydrogenation is often used as criteria to evaluate selectivity ([Sun et al., 2018](#)).

The main reaction of PDH is strongly endothermic and increases in total moles of gas, thus lower partial pressure benefits the appropriate conversion. The high temperature is also necessary for breaking the limits of thermal balance. To maximize propylene generation, temperature needed in PDH reaction is about 550–700 °C ([Yang et al., 2012](#)). It is noted that some other methods are used to break through the limit of thermodynamics, such as oxidative dehydrogenation ([Atanga et al., 2018](#)) (the addition of CO₂, O₂ or other oxides into reaction gas to increase the conversion by removing H₂), adsorbed membrane reactor([James et al., 2016](#); [Kim et al., 2016](#)) (remove H₂ by membrane exchange) and partial

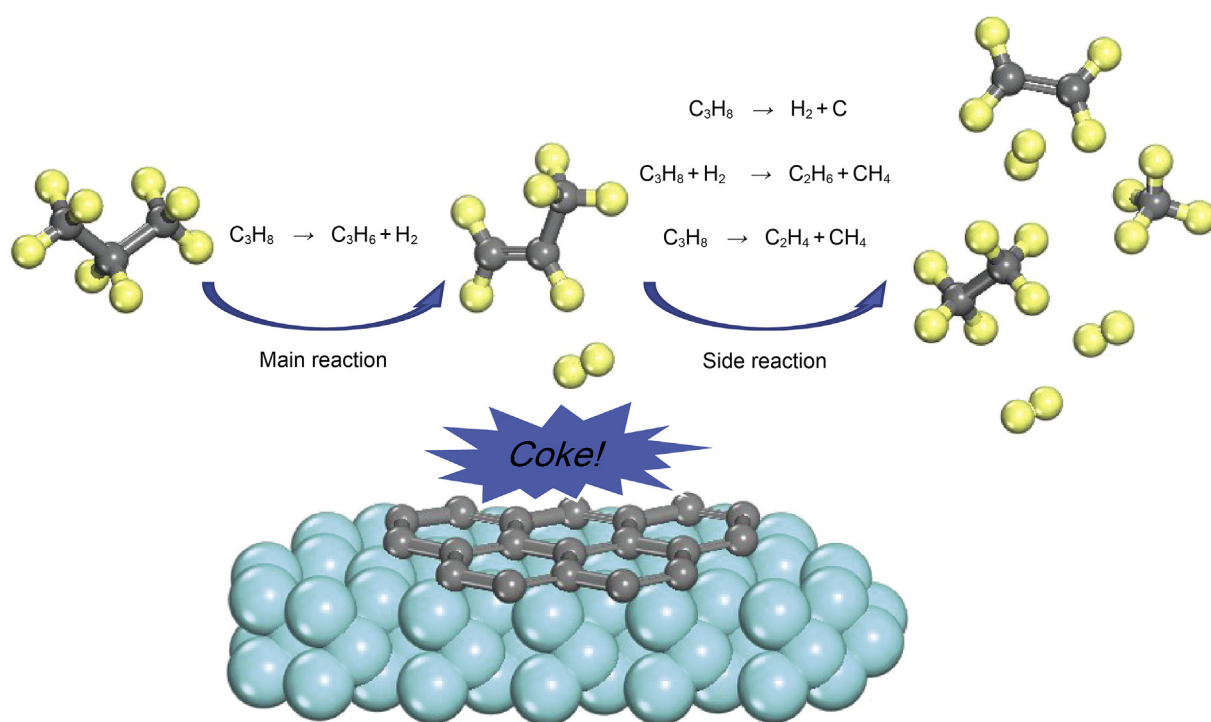


Fig. 1. A simplified reaction condition of propane dehydrogenation and its side reaction (the yellow balls are hydrogen atoms, the gray balls are carbon atoms, and the blue balls are abstract active sites).

alkane combustion, however, they all have their own limitations and have not been used in industrial propane dehydrogenation. (Kong et al., 2020).

In summary, for PDH, fracture of C–H bonds is the focused question. Catalyzing cleaver of C–H bonds is an important organic reaction. For heterogeneous catalytic cleavage of C–H bond, its mechanism is often considered as oxidation mechanism or electrophilic mechanism and could be catalyzed by oxide or metal catalysts (Lillehaug et al., 2004). For alkane dehydrogenation, after a long screen in the past, PtSn- and Cr-based/ Al_2O_3 catalysts have been applied in industrial application (Nawaz, 2015). Other catalysts, such as Ga (Yu et al., 2020; Im et al., 2016), V (Wu et al., 2017), Zn (Camacho-Bunquin et al., 2017; Schweitzer et al., 2014), Zr (Otroschenko et al., 2017), Sn (Wang et al., 2016), Fe (Tan et al., 2016) based-catalysts, are also widely studied and may be competitors for applications in the future. However, they all have their own limits in stability, selectivity and conversion. Deep understanding structure-activity relationship of metal and oxide catalysts is very important to improve catalytic performance. During reaction condition, the formation of coke deposition and the adsorption of gaseous species also have important influence on the structure of the catalyst.

3. Metal catalysts

3.1. Development status and nature of active sites

VIIIB metals have good performance in catalyzing dehydrogenation reaction. Among them, Pt has the best catalytic performance (Sattler et al., 2014). Pt-based catalysts have excellent one-way stability, high selectivity and undoubtedly first-class activity, which provide great convenience to product separation and long-time continuous reaction. The industrialized PtSnK/ Al_2O_3 catalysts have stability up to several hours and high selectivity, which has been used to provide high purity propylene for polypropylene industry (Sattler et al., 2014). The whole process is powered by a semi-continuous interstage heater and regenerated dynamically in moving bed for maintaining a uniform propylene outlet flow rate. Another famous Pt-based catalyst developed by Uhde co-feed steam and thus further improve anti-coke stability (Nawas et al., 2015). However, high-level price still limits widely utilization of Pt-based catalysts in PDH. Pt has almost 100 times higher price than elements used in oxide catalysts. In general, loading of Pt is need to be controlled lower than 1 wt% to maintain its economic benefits. Recently, the latest platinum-based catalyst of UOP even has only a 0.3wt%Pt loading (Ji et al., 2020). Cost-efficient has been the key challenges for Pt-based catalysts. At the same time, pure Pt-based catalysts always have low selectivity and suffered by coking and sintering, it is necessary to improve the supports, promoters and synthesis methods (Liu and Corma, 2018) (Liu et al., 2019). Except Pt, other VIIIB metal catalysts due to their lowly intrinsic selectivity or poor activity are less used in PDH. However, some of them have higher C–H cleaver activity and lower price than Pt, this gives them great potential in future (He et al., 2018).

For metal catalysts, the whole PDH reaction could be catalyzed by metal cluster from multiple atoms to even single metal atom theoretically (Yang et al., 2011). A whole adsorption diagrams during dehydrogenation and deep dehydrogenation are shown in Fig. 2a. Reaction mechanism of PDH in metallic catalysts is widely recognized as a reverse Horiuti–Polanyi (HP) mechanism, which could be divided into four steps (Sattler et al., 2014): Propane would firstly adsorb on surface of metal thought a weak physisorption drove by van der Waals force. (Lian et al., 2018; Yang et al., 2010). Then, two adjacent C–H bonds on propane are successively dissociated by two adjacent metallic atoms. Finally, propylene and H_2

desorbed from metal surface. Two C–H cleaver steps always have the highest energy barrier in this mechanism, thus PDH is also widely considered as a surface reaction-controlled process follows Langmuir–Hinshelwood kinetics.

While main reaction could occur on single metallic atom, undesired reaction step such as deep dehydrogenation and cleaver of C–C bonds in PDH need more adjacent active sites. (Yang et al., 2011). Hydrocarbons adsorbed on metal surface would more like retain their alkane structure (Yang et al., 2010). For example, propylene adsorb on Pt (111) face though di- σ bonds, these bonds would still keep their SP^3 hybridization structure. While the hydrogen atoms continuously dehydrogenate from propane, in order to maintain original coordination morphology of propane, more consecutive sites are favored (Lian et al., 2018). Pure metal catalysts due to their multiple sites always would suffer severe side reaction. (Pham et al., 2016). Generally, 3-fold active sites are considered to be the smallest site that could catalyze the side reactions effectively (Zhao et al., 2015) Purdy et al. (2020) synthesized a variety of Pd-based catalysts alloyed with different promoting metals including Zn, Ga, In, Fe and Mn. As showed in Fig. 2b, Pb atoms in PbZn and PbIn alloy nanoparticle catalysts only exist as the isolated Pb sites and thus have the highest selectivity. Pb_3Fe and Pb_3Mn alloy have relatively lower selectivity because of the presence of three-fold Pb sites. For Pb_3Ga alloy, although 3-fold Pb sites exist, the positive triangle structure of threefold Pb ensemble is distorted by alloying, so it has higher selectivity than Pb_3Fe and Pb_3Mn . This result reveals the importance of site continuity for selectivity.

The coordination environment of metal atoms also plays important role. Defects in end of atomic arrangement, such as the edges or corners, have low coordination number and high electron deficiency. These unsaturated coordination metal atoms strongly adsorb reactants and is more preferred to dehydrogenation and deep dehydrogenation. Size or structure of nanoparticles would affect amounts of defect directly. Zhu et al. (2015) synthesized a serious Pt/Mg(Al)O catalysts with different particle size from 1 nm–10 nm for PDH. They found sample with medium particle size shows the highest propylene formation rate. When particle size increases, propylene selectivity increase but conversion rate of propane decreased, which result a volcano curve relationship between particle size and propylene formation rate showed in Fig. 2c. Author think this structural-sensitivity-like phenomenon is attributed to the surface of small platinum particles have more unsaturated step atoms which not only have a higher dehydrogenation activity but also stronger C–C cleavage tendency than terrace atoms (Nykanen et al., 2013).

In sum, the continuity and coordination environment of metal active sites play important role in catalytic performance. Nature of active sites in metal catalysts could be regulated by the interaction of other components such as promoters and supports. Addition of second metal could alloy with active metal, resulting metal-metal bonds could adjust catalytic performance. Support provides adsorption sites and surface area available for dispersing metal particles. In some cases, interfacial area between support and metal also plays complex electronic and geometric interaction. Next two parts, we would outline these structure-activity relationships in detail.

3.1.1. The role of promoters

Pure metal catalysts always have low selectivity and suffered by serious coking and sintering. Alloyed with second promoting metal could effectively modify catalytic performance from ensemble and electronic effect. Sn is the most used promoter in Pt-based catalyst and famous as industrial promoter used in commercial PtSnK/ Al_2O_3 catalysts. It has been widely reported that the addition of Sn could

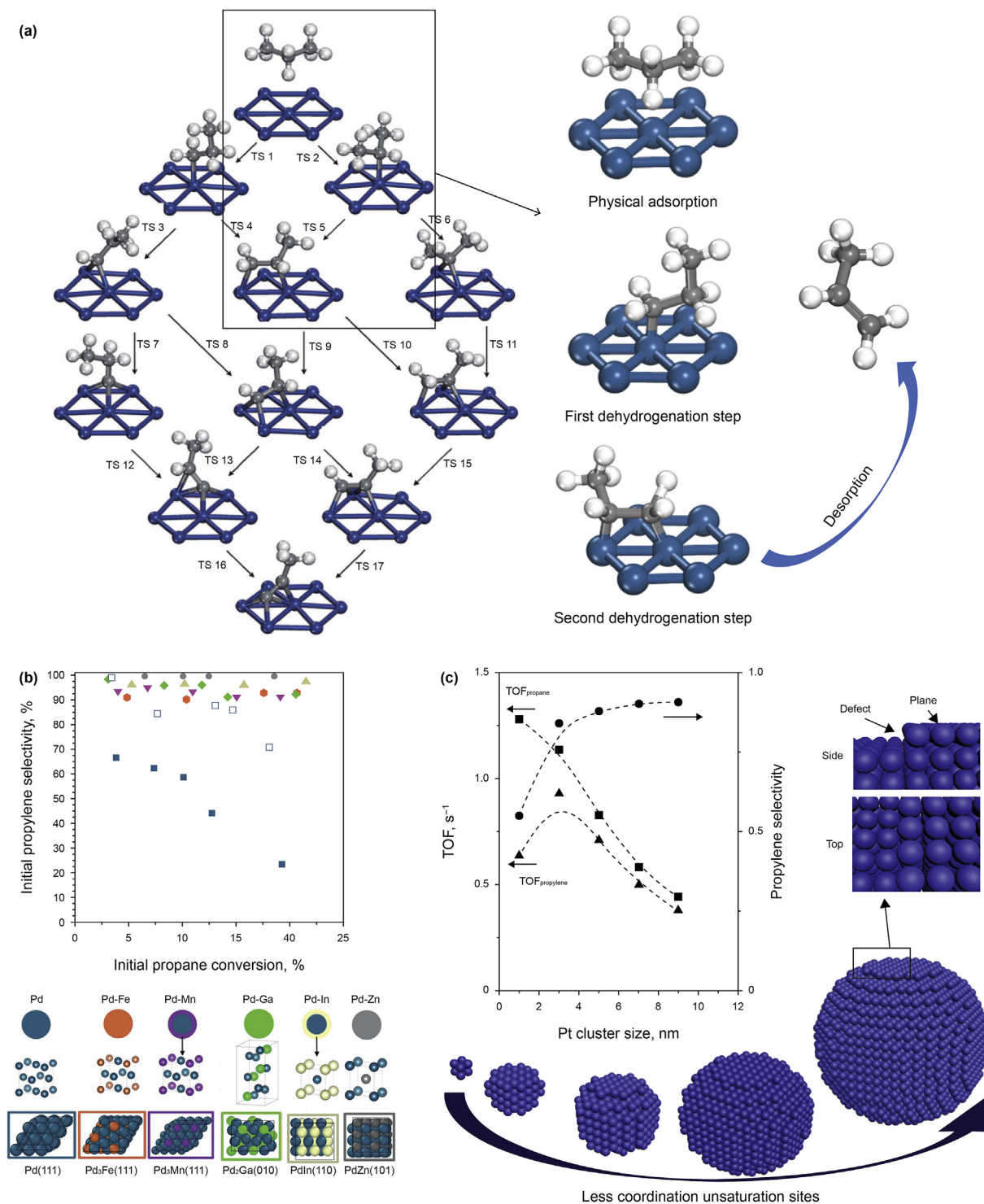


Fig. 2. (a) The reaction mechanism of metal catalysts for PDH reaction. The picture shows propane dehydrogenation reaction on Pt (111) surface (Yang et al., 2011). (b) Effect of aggregation state of Pd atoms from atomic surface to trimer and isolation site on the selectivity (Purdy et al., 2020). (c) Relationship between selectivity, conversion and size of Pt nanoparticles (Zhu et al., 2015).

restrain side reaction and improve catalytic conversion (Pham et al., 2016; Wang et al., 2019). In-situ characterization techniques have identified transformation of chemical state of Sn from oxide state to metallic state and Sn atoms move into platinum lattice forming Pt–Sn alloy during the PDH process (Deng et al., 2014; Iglesias-Juez et al., 2010; Kaylor and Davis, 2018). However, microscopic interaction between Sn and Pt in nanoparticle is still illusive due to

complexity of real alloying metal particles. Ensemble effect and electronic effect has been used to explain the role of Sn. Electronic effect thinks Sn atoms would play its role as an electronic donor and increase the electronic density of 5d band of platinum atoms, enrichment of this electronic state benefit rapid desorption of propylene due to repel force between electron-rich π bonds in propylene and metal surface (Deng et al., 2018; Long et al., 2016).

Ensemble effect think non-reactive Sn atoms would dilute large platinum ensembles into small clusters by formation of alloy and thus increased the selectivity of the reaction due to structural sensitivity of side reaction in PDH (Zhu et al., 2014; Zhu et al., 2017).

For explaining role of Sn, the researchers have made a lot of effort in modeling ideal surfaces and DFT calculation. Yang et al. (2012) performed a DFT research of dehydrogenation of propane on Pt, Pt₂Sn₁ and Pt₃Sn₁ (111) face for explaining the ensemble and electronic effects of Sn in various surface of Pt–Sn alloy. Authors found that the Sn atom causes a downshift of d-band center of adjacent platinum atoms, which results in the weaker bond between carbon atoms of hydrocarbon and Pt atoms. However, downshift of d-band center also improves energy barrier of dehydrogenation step, thus lead to decrease in conversion. Results of calculation also indicate Pt₃Sn bulk is the most suitable alloying surface. Another explanation think Sn atoms would preferentially cover and deactivate Pt atoms in edge, corner which are electron deficient and are apt to catalyze side reaction (Virnovskaia et al., 2007). Nykänen and Honkala, 2013 compared the PDH performance on step sites of pure Pt (211) and Pt₃Sn (211) face in which Sn atoms located on the step edge of platinum based on DFT. In Fig. 3a, as the Pt (211) step sites with coordination unsaturation would adsorb propylene tightly, after decorated by Sn, Pt₃Sn (211) edge would have a obviously weaker bond with propylene. Sn atom located at edge significantly inhibited deep dehydrogenation and weaken propylene adsorption, and improve selectivity. For understanding catalytic process in experiment, well-defined Pt–Sn alloy surface for experimental verification are also ongoing to provide a better understanding. Zhu et al. (2014) synthesize a series of Sn surface-enriched Pt–Sn nanoparticles through a surface organic chemistry (SOMC) method and support them on MgAl₂O₄. As shown in Fig. 3b, with the increase of Sn usage, the surface of nanoparticles gradually appears an enrichment of Sn and form spherical shell-like structure, while the particle size remains unchanged. With the process of Sn surface enrichment, the selectivity and conversion gradually increase. It is directly proved that isolation effect of Sn has an important effect on the PtSn catalysts.

Although the electronic and ensemble effect have successfully explained many experimental phenomena in PtSn catalysts, these studies are only limited to the surface of PtSn nanoparticles. Under really experimental conditions, the interaction between Sn and Pt is far beyond surface interaction, the difference between the inner and outer layers in alloy could still cause large difference in reaction performance (Wu et al., 2018). Ye et al. (2020) synthesized a series of PtSn@Pt/SiO₂ catalysts with a well-defined Pt₁Sn₁ surface. With the increase of the number of subsurface Pt–Sn coordination bonds, the selectivity almost remains unchanged while the TOR continue increasing. Therefore, author considered that the isolated effect by surface Sn atoms mainly affect selectivity, while the TOR is more related to electronic effect of subsurface Sn. The structure-performance relationship is shown in Fig. 3d. It can be seen that the surface and internal structure of Pt–Sn catalyst have important effects on the catalytic performance.

In addition, Sn element has many other effects on Pt-based catalysts. Pham et al. (2016) studied the structural changes of Sn of PtSn/ γ -Al₂O₃ in regeneration-reaction process and found interaction between Sn and Al₂O₃ would play an important role. After the process of oxidative regeneration, Sn would de-alloy from Pt–Sn nanoparticles and anchor on the Al₂O₃ support as Sn atoms or clusters. These adsorbed Sn sites provide nucleuses for recreation Pt–Sn nanoparticles. Therefore, Pt–Sn catalysts would recover their own high dispersion after redox process used Al₂O₃ as support, while the size of pure-Pt catalysts will continue increasing after several regenerations. Although the traditional idea is that Sn can only improve the activity of catalyst in the form of alloy, recent

studies have shown Sn in oxide state could also improve the catalytic performance and like a strong metal-support interaction (SMSI). Deng et al. (2018) reported a SMSI effect between Pt and SnO_x in Pt–Sn/SiO₂ catalysts. Traditionally, Sn is pretreated by H₂ to form an alloy structure though ensemble and electronic effect, author found Sn in Pt–SnO₂/SiO₂ pretreating by O₂ and N₂ would play similar role, even all Sn species are only existed as SnO₂. A more detailed structure modeling and comparison of catalytic performance is shown in Fig. 3c. Compared with the Pt catalyst without Sn, the electronic state of Pt with SnO_x was effectively increased after pretreatment of nitrogen, resulting in the improvement of selectivity and conversion. Identify promoting role of Sn still needs to further researches.

Other metals, such as Ga (Bauer et al., 2019), Zn (Rochlitz et al., 2020) and In (Xia et al., 2016), Cu (Ren et al., 2018; Han et al., 2014), V (Purdy et al., 2020), Co (Cesar et al., 2019), Mn (Wu et al., 2018; Fan et al., 2020) and Fe (Cai et al., 2018), are also widely used in Pt–M catalysts (M stands for promoting metal) and their role of promoters are always explained like Sn. Nakaya et al. (2020) synthesized a novel PtGa–Pb/SiO₂ ternary alloy catalyst with isolated Pt atom structure. In the surface of PtGa nanoparticles, Pd atoms would selectively locate on threefold Pt sites driving by thermodynamic effect and only keep isolated Pt active sites. PtGa–Pb SAAC has higher stability and selectivity than the sample without Pb. X Sun et al. (2018) synthesized a novel kind of PtCu Single-atom alloy catalyst (SAAC). By addition of Cu, Pt ensembles were dispersed to isolated single-atoms. PtCu SAA has a similar TOF but higher selectivity than pure Pt catalyst. DFT calculation shows that the Pt atom dehydrogenation activity on Pt–Cu alloy is almost unchanged, but the propylene desorption ability increases significantly which prevent deep dehydrogenation and other side effects. By precisely controlling solid state transformation of Mn atom into Pt nanoparticles, Wu et al. (2018) synthesize and identified Pt@Pt₃Mn core-shell nanoparticle catalysts and pure Pt₃Mn nanoparticle catalysts. The selectivity of Pt@Pt₃Mn is effectively lower than that of Pt₃Mn alloy. DFT calculation indicated Mn atoms in the subsurface would reduce the surface adsorption of propylene, thus inhibit side reaction. Interaction between these various promoters and platinum still needs more extensive study.

Except Pt, other VIII B metals could also be modified by second promoting metals. Ni, Co, Fe metals have higher dehydrogenation activity than Pt, but prone to generate cracking products or coke than producing propylene. (Chen et al., 2020; Saelee et al., 2018). Some other noble metals, such as Pd, Rh and Ru, have also been used in PDH because of similar electronic and geometric structures to platinum (Ma et al., 2020; Purdy et al., 2020; Natarajan et al., 2020). Addition of appropriate promoters has potential to improve these essential shortcomings. He et al. (2018) synthesized a Ni–Ga nanoparticle catalyst supported by Al₂O₃ (70% delta, 30% gamma phase). This alloying NiGa catalyst had a high initial selectivity of 94% and long-term stability, while pure Ni has a poor selectivity approached to 0 and bad stability due to serious coking deposition. For studying the effect of Ga on Ni deeply, researchers further synthesized a series of catalysts with different Ni:Ga surface ratio. Higher surface gallium content is main reason of the high selectivity in NiGa/Al₂O₃ catalyst. Raman et al. (2019) studied performance of RhGa/Al₂O₃ catalyst in PDH. Addition of Ga would form solid intermetallic phases with Rh and improve catalytic performance. Continuing to increase amount of gallium would result in gradual formation of Rh–Ga liquid metal solutions and a sharp rise in selectivity and activity will be observed while alloy is all liquid state. DFT showed present a synergistic effect between Ga and Rh, activation of propane is happened on single-atom Rh and has formed propylene would diffuse and desorb from Rh to the Ga, and it may be the reason of high activity of isolated Rh atom.

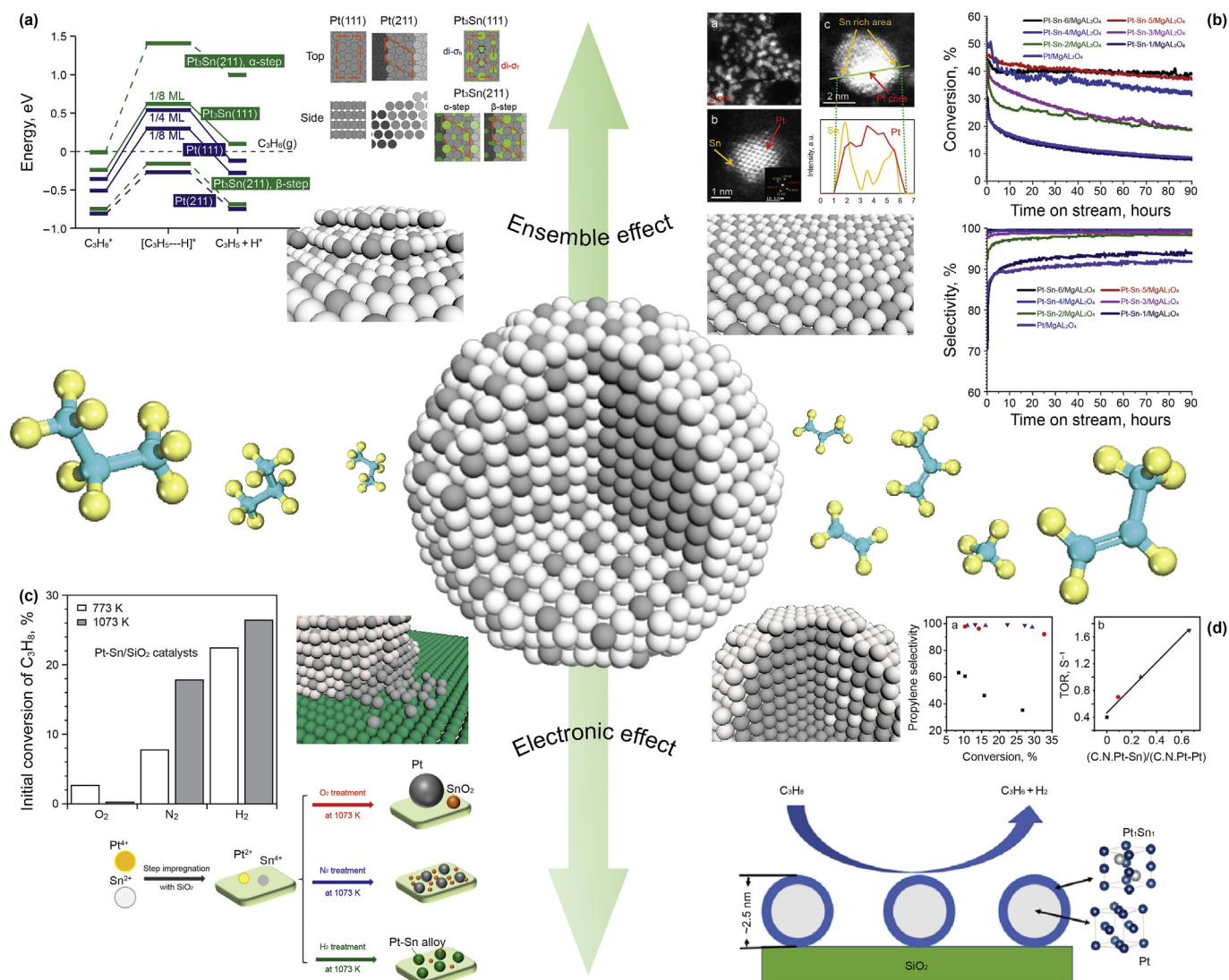


Fig. 3. The role of Sn and other metal promoters in Pt-based catalysts for PDH reaction. (a) Sn atoms covered unsaturated platinum atoms (Nykänen and Honkala, 2013). (b) Sn and Pt form intermetallic alloy (Zhu et al., 2014) (c) SMSI effect between SnO₂ and Pt particles (Deng et al., 2018) (d) Electronic interaction of sub-surface Sn atoms in Pt–Sn core-shell catalysts (Wu et al., 2018).

3.1.2. The role of supports

For metal-based catalyst, the role of the support is dispersing metal particles and avoiding the irreversible sintering at the high temperature of PDH. Support with high surface area is obviously benefit to disperse and stabilize uniform and ultra-fine metal particles. In addition, appropriate pore diameter which is matched to particle size would show higher resistance to sintering which is also called confinement effect. Because of the above property, aluminum and silicon-based supports with higher specific surface area and adjustable pore structure are widely used in metal-catalyzed PDH process, and ordered mesoporous materials and microporous molecular sieves have unique advantages in stabilizing nanoparticles though confinement effect. In terms of support-metal interaction, supports used in PDH are usually electrically inert and hardly reduction for avoiding undesired side reaction or structural collapse, coordination unsaturated defect on these non-reducible oxide support would provide strongly local-unsaturated adsorbed sites to anchor these metal particles (Ji et al., 2020; Kwak et al., 2009). Thus, adjusting the surface defected sites are important in improving metal particles dispersion and stability.

Among aluminum-based materials, γ -Al₂O₃ is the most common commercial support, which has low price, high thermal stability and strong resistance to abrasion (Sattler et al., 2014). In the surface of γ -Al₂O₃, coordinatively unsaturated pentahedral coordination Al³⁺ could anchor metallic component and prevent metallic nanoparticles aggregation (Gong and Zhao, 2019; Yu et al., 2020; Kwak et al., 2009). The amounts of unsaturated coordinated sites are closely related to the preparation method and morphology. Shi et al. (2015) synthesized a novel PtSn/Al₂O₃ sheet catalyst for PDH. Rich-defected Al₂O₃ sheet would attribute to more unsaturated pentahedral Al³⁺ sites than commercial γ -Al₂O₃, and thus effectively stabilize ultra-small raft-like Pt–Sn clusters. PtSn/Al₂O₃ sheet catalyst has an extraordinary selectivity up to 99% and only suffered trace deactivation happened during 24h reaction test. Sheet-like structure also has a positive impact on mass transfer, and benefit better activity and selectivity at high space velocity. Gong and Zhao, 2019 synthesized a novel peony-like alumina nano-sheet (Al₂O₃-MG) with richer pentahedral Al_(III) by glucose-assisted hydrothermal method and supported PtSn catalyst on it. The strong interaction between pentahedral Al_(III) sites and PtSn nanoparticles

improved anti-sintering ability, thus, PtSn/Al₂O₃-MG catalyst has an unexcepted stability and conversion.

Although γ -Al₂O₃ is good for achieving high dispersion of metal particles, however, acid sites on Al₂O₃ surface would catalyze undesired coke deposition and cracking reaction. Introducing basic promoters to adjust surface acidity is common solution. Addition of K, Na et al. alkali metal would partially cover the strong acidic sites and result in the reduction of side reactions (Sattler et al., 2014a). Other basic oxide such as Mg, Zn, Ca and some rare earth elements (Vu et al., 2016; Im et al. 2016) are also widely used for similar purpose. In addition to adjusting acidity, formation of MgAl₂O₄, ZnAl₂O₄ Spinel phase after addition of Mg, Zn would provide additional anchoring effect on metal particles by epitaxial metal-oxide interfacial caused by similar structure with Pt (111) face (Belskaya et al., 2016). Ren et al. (2018) systematically studied the promoting role of IB metals in Pt-M/MgAl₂O₄ and effect of MgAl-spinel on propane dehydrogenation. Compared with γ -Al₂O₃, although the original size of particle in both supports are very similar, MgAl₂O₄ evidently provide a stronger interaction to Pt nanoparticles and showed a better reaction-regeneration performance in multiple regeneration. After the introduction of IB metal promoters (Cu, Ag, Au), selectivity and conversion of all Pt-M catalysts have improvement, among them Cu has the most preferred promoting effect. This may due to worse affinity with Pt of Ag and Au, and thus result in formation of amorphous alloy, while Cu would form stable Pt–Cu intermetallic alloy with high stability and better dispersion. Some low melting-point oxides are also used in propane dehydrogenation to partially cover the acidic sites on the surface of alumina. Aly et al. (2020) found that introducing B species into Pt/Al₂O₃ catalysts can a reduction of coke formation and side reaction. DFT calculation indicated formation of finely dispersed amorphous B₂O₃ on alumina, which covered stronger acid sites on Al₂O₃ and reduce unwanted side reaction. The improvement of alumina-based support still needs further more exploration and research.

Except for aluminum-based materials, pure silica materials, especially pure silica zeolites, have been widely studied in the field of PDH because of their low acidity, high specific surface area and adjustable, homogeneous and ordered pore structure. However, inert property of silica material also leads weak adsorption capacity. At preparation process, due to the lack of strong electronic attraction, metal precursors could be often evenly distributed on the surface of silicon oxide (Fan et al., 2020). At the reaction and regeneration process, due to the lack of strong adsorption sites, oxidized metal particles would suffer intensive sintering (Kaylor and Davis, 2018). Therefore, the research on silicon materials mainly focuses on improving the interaction between support and metal in both preparation and reaction-regeneration process.

Creating the adsorbed sites on SiO₂ materials by metal doping is a very common method to produce adsorption sites for metallic nanoparticle. Fan et al. (2020) used MnO_x modified mesoporous silicon nanoparticle as a support to disperse platinum. The modified of MnO_x provide strong electron adsorption to Pt precursors thus result better dispersion of Pt. Moreover, metallic Mn produced from reduction also play promoting role though alloyed with Pt. DFT calculation shows that the formation of PtMn alloy not only promote the propylene desorption, but also can keep a good activity of initial dehydrogenation. For zeolite support, although presence of aluminum atom provides additional anchored effect to metal particle, caused strong acidity would lead to serious coke deposition. Many studies have tried to exchange the framework structure of silica-alumina zeolite with other metals like Zn (Zhang et al., 2015), Sn (Li et al., 2017), Ti (Li et al., 2017), Fe (Waku et al., 2003) to obtain a relatively low acidity but keep stronger interaction. Zhang et al. (2015) synthesized a Zn-ZSM-5 zeolite though use

Zn precursor instead of Al precursor. Compared with the traditional Al-ZSM-5, the Zn-ZSM-5 has lower acidity which reduce coke deposition. At the same time, Zn also provide a strong interaction than Al-ZSM-5. Formation of Pt–Zn nanoparticles also improve selectivity and conversion.

Except for the introduction of heteroatoms, surface organometallic chemistry method (SOMC) also provides an optional method to directly anchoring stable metal nanoparticles by pure silicon material. Although silicon oxide materials due to its electric neutrality could not provide strong adsorption capacity for metal precursors in water through the electric attraction, hydroxyl groups on the surface of SiO₂ can be connected with metallic organic precursors by SOMC and form highly dispersed even isolated metal sites (Xu et al., 2019). Searles et al. (2018) prepared a novel PtGa/SiO₂ catalyst via grafting Pt and Ga precursor onto the surface of silica gel and form Ga and Pt single-sites, after reduction, they obtained homogeneous and ultrasmall Pt–Ga alloying nanoparticles. This catalyst had amazing catalytic performance which high conversion (31.9%), selectivity (99%) by only usage of only 0.001g catalyst in a very high space velocity with ultrahigh stability and regeneration ability. Two different kinds of Ga species were observed in PtGa/SiO₂: metallic Ga and remained single Ga³⁺ on SiO₂. Metallic Ga formed bimetallic particles with Pt thus the selectivity and stability is improved. In addition, isolated Ga³⁺ on the surface of SiO₂ is related to formation of strong Lewis acid sites, which may enable to the nucleation and stabilization of ultra-small Pt–Ga nanoparticles. Another PtZn/SiO₂ catalyst which has similar synthesis method was also prepared by Rochlitz et al. (2020) PtZn/SiO₂ catalyst has also a high conversion, selectivity, stability like mentioned-above PtGa/SiO₂ catalyst. The formation of Pt–Zn alloy is considered as an important reason to the high selectivity of PtZn/SiO₂.

Through dealumination of Si–Al sieves, the silanol nest formed after dealumination on sieve has strong adsorption capacity than common silica material, these sites could effectively disperse metal precursor sites at the initial stage of preparation. Xu et al. (2019a,b) further introduced this SOMC method into the synthesis of PtSn catalyst supported by dealuminated beta zeolite. Though directional interaction between organic functional group, isolated Sn atoms would localize in the framework of beta zeolite and prefer to form smaller PtSn clusters with Pt. PDH test showed that the Pt/Sn2.00-Beta catalyst had the highest conversion (50%) and selectivity (99%). It is worth noting that similar stable Pt clusters have been obtained by the same method on Y zeolite, which indicates that this method may be a general sintering inhibition method to Silica alumina zeolites. Ryoo et al. (2020) co-impregnated Pt(NH₃)₄NO₃ and nitrate ions of rare earth in the de-Ga molecular sieve. Silanol nest formed by dealumination would stabilize rare earth ions exist in the form of single atom and thus easy to be reduced. After reduction treatment at 700 °C in H₂, rare earth metal-platinum alloy catalyst was obtained. This catalyst has high selectivity, conversion and shocking stability up to several days.

Encapsulation of Pt–M clusters into micropores of zeolite by in-situ method or post-synthesis could also synthesize ultrasmall Pt alloyed cluster and effectively inhibit sintering due to confined effect. Wang et al. (2020) synthesize a novel PtZn@S-1 catalyst via hydrothermal method. XPS found some of the Zn species exist as Zn²⁺ and located into lattice of S-1 zeolite, and others form Pt–Zn alloys with Pt species. Ultrasmall Pt–Zn alloys particles with high catalytic performance are encapsulated inside S-1 zeolite though in-situ synthesis. The confinement effect of S-1 channel effectively prevents the sintering of Pt–Zn particles. Liu et al. (2020) synthesized a novel K–PtSn@MFI catalyst. Through XAS, TEM, author proved sub-nano Pt clusters(0.6 nm) are confined in the sinusoidal 10R channels of MFI. Interaction between Pt and Sn can be

effectively controlled by adjusting the reduction method. Increasing the reduction temperature or time could help Sn to enter into Pt clusters and provide promoting effect, thus increasing selectivity and slowing down deactivation rate. Under a condition similar industrial process, the K–PtSn@MFI catalyst exhibited a selectivity of up to 97% and an initial conversion of 20% with only 3% deactivation in 70h.

The traditional supports such as Al₂O₃ and SiO₂ are electric inertia generally interact with metals by local defect sites. Although these defects have some anchoring effects, but they still failed to provide more effective electronic interaction with Pt. Therefore, some supports which provide strong metal-support interaction (SMSI) have received the much attention from researchers. The SMSI effect provides additional electronic interaction and modify interface structure between support and metal, thus it is expected to an interesting way to change catalyst performance. (Liu et al., 2020). Jiang et al. (2014) studied the promoting role of TiO₂ on Pt/Al₂O₃ catalyst. After doping Ti into Al₂O₃, both selectivity and conversion have obvious improvement, despite Pt/TiO₂–Al₂O₃ and Pt/Al₂O₃ has similar particle size of about 2 nm. This phenomenon may be due to SMSI between TiO₂ and Pt would increase electronic density of Pt atoms. Electron-rich Pt promote desorption of propylene and prevent side reaction. A high electronic density also weak attachment of coke precursor, so promote migration of coke from metallic nanoparticles to support. Liu et al. (2017) synthesized a novel Pt/ND@G (graphene shell in nano diamond) catalyst which has high selectivity (90%) and shows slight deactivation in 100h. The electron transfer from defective graphene to platinum nanoparticles improved anti-sintering ability of Pt/ND@G. In addition, this electron transfer also increases electronic density of Pt surface and inhibit coke deposition and side reaction effectively.

In regeneration process of PDH, treating catalysts with high temperature air would oxidize part Pt⁽⁰⁾ to volatile Pt²⁺, Pt⁴⁺ species, and finally lead agglomerate (Kaylor and Davis, 2018; Pham et al., 2016; Xu et al., 2018; Uemura et al., 2011). A strong interaction between Pt species and support under air condition is also important to inhibit sintering in regeneration process. CeO₂ is well known for its special trapping platinum atom ability in high temperature. Xiong et al. (2017) synthesis a novel PtSn/CeO₂ catalyst. The strong interaction between Pt and CeO₂ effectively minimized sintering of small Pt–Sn clusters. Interestingly, during the oxide regeneration process, Platinum clusters supported on CeO₂ would be dispersed into single-atoms. In reduction period, the dispersed Pt atoms will be self-reassembled to Pt–Sn cluster and restore original dispersion, while in Pt/Al₂O₃ Pt particle would aggregate violently after regeneration. This self-assembly process is shown in Fig. 4. Xu et al. (2018) added β-Ga₂O₃ with different shapes to Pt/Al₂O₃ and studied their influence on propane dehydrogenation. PDH results suggest Ga₂O₃ can stabilize the particle size of platinum in air at high temperature. This may be because Pt particles could be captured by Ga₂O₃, which prevents Pt from being oxidized into PtO_x large particle. Recent catalysts are shown in Table 1.

4. Oxide catalysts

4.1. Development status and nature of active sites

Oxide catalysts in PDH could be divided into supported catalysts and bulk catalysts. Compared with Pt, oxide catalysts have their own advantage such as significantly lower price and convenient regeneration process, while Pt catalysts need using dangerous Cl₂ to redispersed large particles (Sattler et al., 2014; Liu et al., 2016; Zangeneh et al., 2015). However, most oxide catalysts are suffered by serious coking deactivation and have much shorter one-way life than Pt catalysts, thus frequent regeneration is necessary (Nawaz

et al. 2015). In industry Catofin technology, CrO_x–K₂O/Al₂O₃ catalysts are regenerated every 10 min, several fixed bed reactors work in turn to keep a constant propylene outflow rate (Sattler et al., 2014). Thus for oxide catalysts, stability during regeneration process always needs to pay more attention than one-way stability. Solid reaction or leaching in regeneration process are culprits of deactivation in regeneration process. For example, in industrial CrO_x/Al₂O₃ catalysts, migration of Cr atoms into framework of Al₂O₃ would form inactive spinel phase and thus lead to irreversible deactivation. The inactivation process can be reduced by selecting supports and promoters properly. In addition, the intrinsic activity of the oxide catalyst is often tens of times lower than metal-based catalysts, which makes the oxide catalyst often need a high loading to achieve appropriate conversion.

Catalytic mechanism of oxide catalysts in PDH is basis on metal-organic chemistry, unsaturated metal-oxide pairs are considered to be the source of active sites. After reduction activation process, Metal oxides would lose a part of oxygen atoms and produce unsaturated metal-oxygen sites, these unsaturated M–O pairs would tend to coordinate with carbon atoms and hydrogen atoms on propane and thus reduce activation energy of C–H cleavage (Chen et al., 2020; Estes et al., 2016; Schweitzer et al., 2014; Conley et al., 2015). In Cr-based catalysts, coordination unsaturated Cr³⁺ and Cr²⁺ reduced from Cr⁶⁺ and Cr⁵⁺ have been widely confirmed as active sites by a series of in-situ characterization (Nawaz, 2015; Santhoshkumar et al., 2009; Puurunen et al., 2001; Gao et al., 2019). Similar to Cr-based system, coordination unsaturated V³⁺ and V⁴⁺ reduced from V⁵⁺ are widely thought as active sites in V-based catalysts (Sokolov et al., 2012; Langeslay et al., 2018; Bai et al., 2016; Zhao et al., 2018; Liu et al., 2016; Xie et al., 2020; Rodemerck et al., 2017). In some cases, the valence of oxides after reduction would not change such as Ga, Zn, but their coordination conditions are changed to unsaturation due to loss of oxygen atom (Sattler et al., 2014). For Ga-based catalysts, tetrahedral (IV) coordination Ga³⁺ reduced from octahedrally (VI) coordinated Ga³⁺ are the main active sites. (Sattler et al., 2014; Schreiber et al., 2018; Choi et al., 2017; Kim et al., 2017; Szeto et al., 2018; Zheng et al., 2005). Although in most oxide catalysts, increasing the reduction degree of the active site could greatly improve its activity due to increase of unsaturation, however, deep reduction is not necessarily beneficial to the oxide catalysts (Sun et al. 2014, 2015; Dai et al., 2020). For example, the active site of Co-based catalyst is considered to be unsaturated Co²⁺O. If CoO_x is reduced to metallic Co nanoparticle, this will result in a sharp decrease in selectivity and stability (Dai et al., 2020). In Zn-based catalysts, Zn metal formed by excessive reduction is inactive and easy to be sublimated and lost from the support due to its low melting point, resulting in irreversible deactivation.

Reverse H–P mechanism is also widely used to describe mechanism of oxide catalysts, but there is a little different in adsorption sites: while physical adsorption completed, propane would be dissociated to alkyl and hydrogen atom, alkyl adsorb on coordination unsaturated metal atoms, while hydrogen atoms adsorb on oxygen atom near these metal atoms. After that, the alkyl would undergo a β-hydrogen transfer and desorbed hydrogen would be adsorbed on metal ions, while propylene adsorbs on the top of metal ions by π-bond (Huš et al., 2020). Then, propylene and hydrogen are desorbed successively (Liu et al., 2016; Estes et al., 2016). This process has been showed on Fig. 5b. The whole reaction is also considered as a surface reaction control mechanism and dehydrogenation step is rate-limited step (Xie et al., 2020; Liu et al., 2016). Although traditional model of oxide catalysts only includes metal-oxide pair M–O and follow HP mechanism, under different chemical conditions, active site structure and reaction mechanism may be different. (Olsbye et al., 2005; Zhao et al., 2018; Dixit et al.,

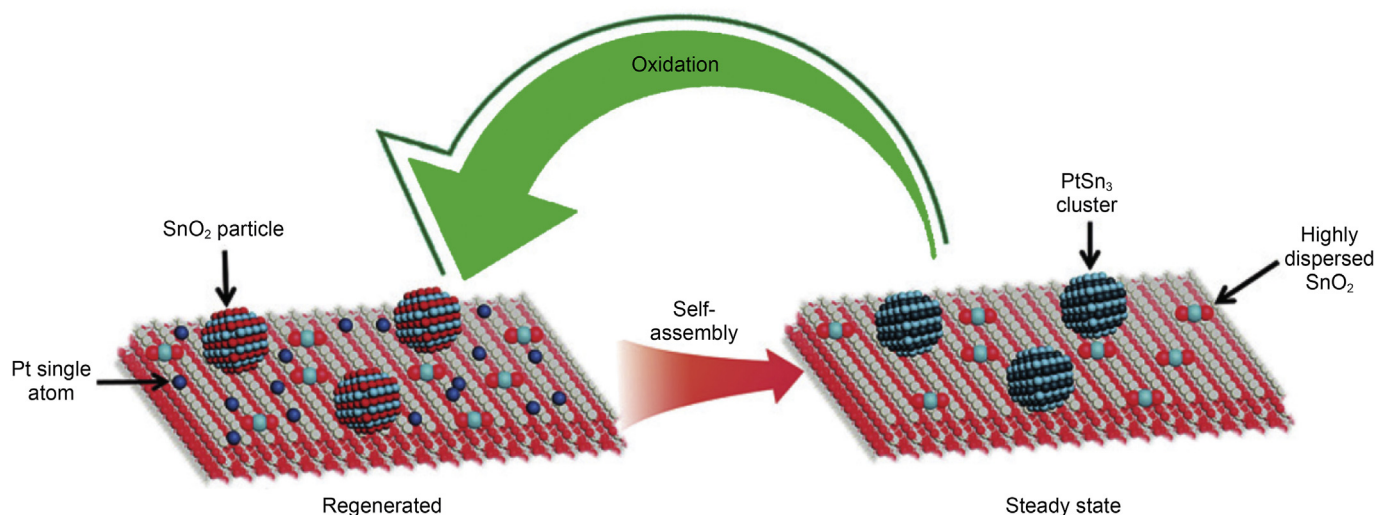


Fig. 4. Self-reassembled process of PtSn/CeO₂ catalysts during regeneration-reaction cycle (Xiong et al., 2017).

Table 1
Catalytic performance of metal catalysts.

Catalyst	Feeding composition	Reaction temperature, °C	Space velocity, h ⁻¹	flow rate, ml/min	Conversion, %	Selectivity, %	Test time, h	Size of catalysts, mesh	Catalyst loading, g	Ref
1Pt6Sn/MgAl ₂ O ₄	Propane:hydrogen:helium = 1:1:8	580	/	20	45–38.9	99.7	90	/	0.05	Zhu et al. (2014)
1Pt1Sn/Al ₂ O ₃	Pure propane	600	WHSV = 3.2	9	35.6	88.5	6	/	0.3	Pham et al. (2016)
0.5 Pt/Mg(Sn) (Al) O@Al ₂ O ₃	Propane:hydrogen:argon = 1:0.5:2	600	WHSV = 14	/	48.3–43	86.4–98.1	48	/	0.4	Zhu et al. (2017)
3Pt1Ga–0.6Pb/SiO ₂	propane:hydrogen:helium = 3.9:5.0:40	600	/	48.9	27–32	99.7	50	/	0.015	Nakaya et al. (2020)
0.6Pt1.5In/Mg(Al)O	Propane:hydrogen:nitrogen = 8:7:35	620	GHSV = 1600	/	58.4–48.6	92.8	30	/	0.3	Xia et al. (2016)
0.5Pt0.5Cu/Al ₂ O ₃	Propane:nitrogen = 1:1	550	WHSV = 3	/	43–42	92	4	/	/	Han et al. (2014)
0.1Pt10Cu/Al ₂ O ₃	propane/hydrogen/nitrogen = 4:4:17	520	WHSV = 4	40	10	90	120	20–40	0.25	(Sun et al., 2018)
0.36Pt0.68Sn/Al ₂ O ₃ sheet	Propane:hydrogen:nitrogen = 1:1.25:4	590	/	50	28.9–27.2	98	24	/	0.1	Shi et al. (2015)
0.5Pt1Sn/Al ₂ O ₃ -MG	Propane:nitrogen = 26:74	600	/	50	37.9–42.2	99.1	35	20–40	0.15	(Gong and Zhao, 2019)
0.5Pt1Na/Zn-ZSM-5	Propane:hydrogen = 4:1	590	WHSV = 3	/	41	91	10	/	2	Zhang et al. (2015)
0.5Pt2Sn/Sn-beta	Propane:hydrogen:nitrogen = 1:1:8	570	WHSV = 2400	/	50–45	92–97	159	/	/	(Xu et al., 2019)
0.4Pt0.9Sn–K@MFI	Pure propane	550	WHSV = 118	/	20–17	97	70	/	0.02	(Liu et al., 2020)
4.3Pt1.7Ga/SiO ₂	Propane:argon = 1:4	550	WHSV = 98.3	/	31.9–17.1	98	20	/	0.001	Searles et al. (2018)
0.3Pt0.5Zn@S-1	Propane:nitrogen = 11:19	600	WHSV = 6.5	/	31–26	99	5	/	0.2	(Wang et al., 2020)
0.5 Pt–Ga ₂ O ₃ rods/Al ₂ O ₃	Propane:nitrogen = 1:9	625	/	100	47–29	92	3	60–80	0.2	Xu et al. (2018)
1Rh125Ga/Al ₂ O ₃	Propane:helium = 1:10	550	GHSV = 4900	/	29	92	15	/	/	Raman et al. (2019)
0.5Co/SiBeta	Propane:nitrogen = 1:19	600	/	20	53.0–40.2	98.2–98.3	6	60–80	0.3	Chen et al. (2020)
3Ni1Ga/Al ₂ O ₃	Propane:argon = 1:9	600	/	20	11	95	82	100	0.1	He et al. (2018)

2018). DFT calculation is of great significance in predicting and interpreting influencing mechanism and detailed information of active sites in oxide catalysts. Zhao et al. (2018) found that pre-treating VO_x/Al₂O₃ by hydrogen could converse V=O bonds on VO_x to V–OH gradually, while pretreating with C₃H₈ would directly lead

to the fracture of V=O. Active sites with V–OH structure have lower activity but slower deactivation (Fig. 5a). With the increase of treating time of H₂, both of the initial activity and deactivation rate would decrease. This also shows the complexity of active sites on surface of oxide. Although the active sites of most oxides are

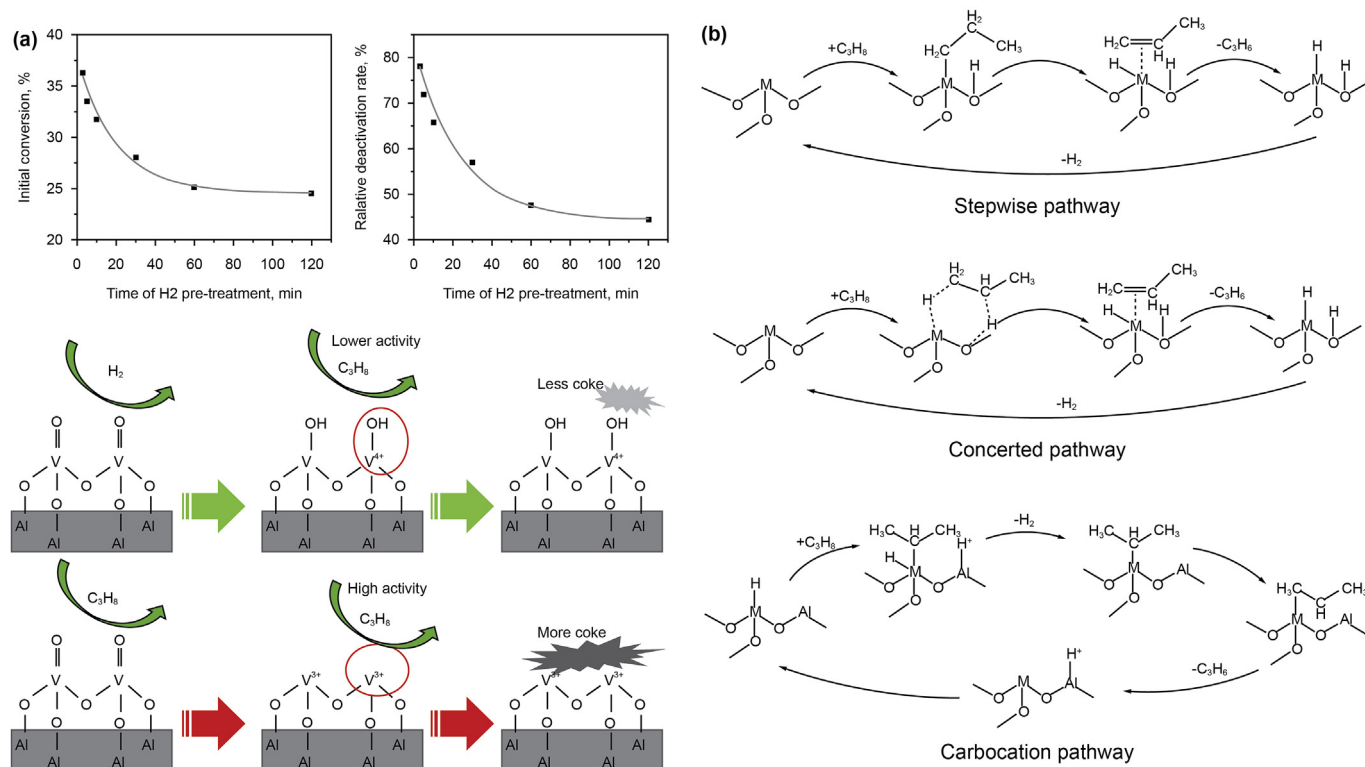


Fig. 5. (a) The relationship between reduction time and conversion, inactivation rate, and the change of active site structure after different reduction methods were also discussed. (Zhao et al., 2018). (b) Several common reaction mechanisms of oxide.

considered to be metal-oxygen pairs, Dixit et al. (2018) made a systematic study in sites with different coordination environment and present of hydroxyl of PDH mechanism on (110) surface of Al_2O_3 by DFT. They also found a volcano relation between binding energy of dissociated H_2 and TOF of PDH. Desorption of H_2 in highest active sites is more suitable to be the rate-limiting step rather than traditional breaking of C–H. $\text{Al}_{\text{III}}\text{–O}_{\text{III}}$ sites of hydroxylated Al_2O_3 (110) which has compromising Lewis acid/base ratio have highest active and follow a concerted mechanism. In addition to alkyl mechanism, mechanism participated with free radicals and carbocation have also been proved to have lower energy barrier in some cases (Mansoor et al., 2018; Lillehaug et al., 2004). Schreiber et al. (2018) found traditional HP mechanism may not be suitable in Ga/H-ZSM-5 catalysts. They indicated while first step of dehydrogenation is still the common heterolytically dissociation process, the second step of dehydrogenation should happen with an intermediate state of carbenium rather than direct cleaver of C–H in alkyl. These mechanisms are listed in Fig. 5b.

In sum, the active sites of the oxides are formed by metal-oxygen pairs after reduction, these sites are often coordination unsaturated. Which oxygen is reduced (M–O–M or M–O–S et al., M is the active metal atom and S is the support), how many oxygen atoms are reduced, and whether forming adsorbed species such as hydroxyl decide the final micro-structure of active sites. In order to modify the reducibility of oxide catalysts, commonly used methods include regulating support and promoter. In addition, supports and promoters also affect the dispersion of active sites in oxide catalysts.

4.2. Aggregate structure and the role of support

Support plays a key role in oxide catalysts for PDH reaction. First and most obviously, support provide landing surfaces for dispersing

active species and effect structure of active sites (Bai et al., 2016). As the intrinsic activity of most oxide catalysts is much lower than that of Pt, a support with larger specific surface area is needed to increase the loading of oxide catalyst in order to achieve higher conversion. However, as increasing loading, polymerized structure of oxide would change from isolated sites to oligomer and finally crystals (Wu et al., 2017) (Fig. 6). The degree of aggregation not only determines amount of exposed active sites, but also plays decisive role in reduction tendency of oxygen atom and active structure during PDH process (Ruiz Puigdollers et al., 2017; Liu et al., 2016; Zhao et al., 2019). A large number of studies in oxide catalysts focus on studying relationship between polymerization state and PDH catalytic performance. Isolated sites are generally considered to have special advantages. They not only have the maximum dispersion theoretically, but also prevent coke precursors contact each other to form graphitized coke (Rodemerck et al., 2017; Liu et al., 2020; Dai et al., 2020; Hu et al., 2015; Hu et al., 2015). Supports with high specific surface area have obviously advantages in keeping them working as isolated sites. Rodemerck et al. (2017) found that in the surface of $\text{VO}_x/\text{MCM-41}$, isolated V sites have the highest activity and coke resistance. Although isolated V species have higher acidity than oligomerized counterparts, the coke precursors are hard to contact with each other and form coke, thus they would have both higher activity and stability in PDH. Synthesis method also plays an important role in dispersing oxide to isolated sites. Traditional impregnation method often leads to the uneven distribution of oxide species, some novel synthesis method such as hydrothermal one-pot method (Dai et al., 2020), sol gel method (Hu et al., 2018) and precursor modification has unique advantages. Zhao et al. (2019) using Zn-based metal organic framework as precursor and synthesized highly dispersed $\text{ZnO}@\text{CN/S-1}$ catalyst. ZnO nanoparticles are highly dispersed and encapsulated into CN material. CN layers effectively hindered the loss of Zn in the high

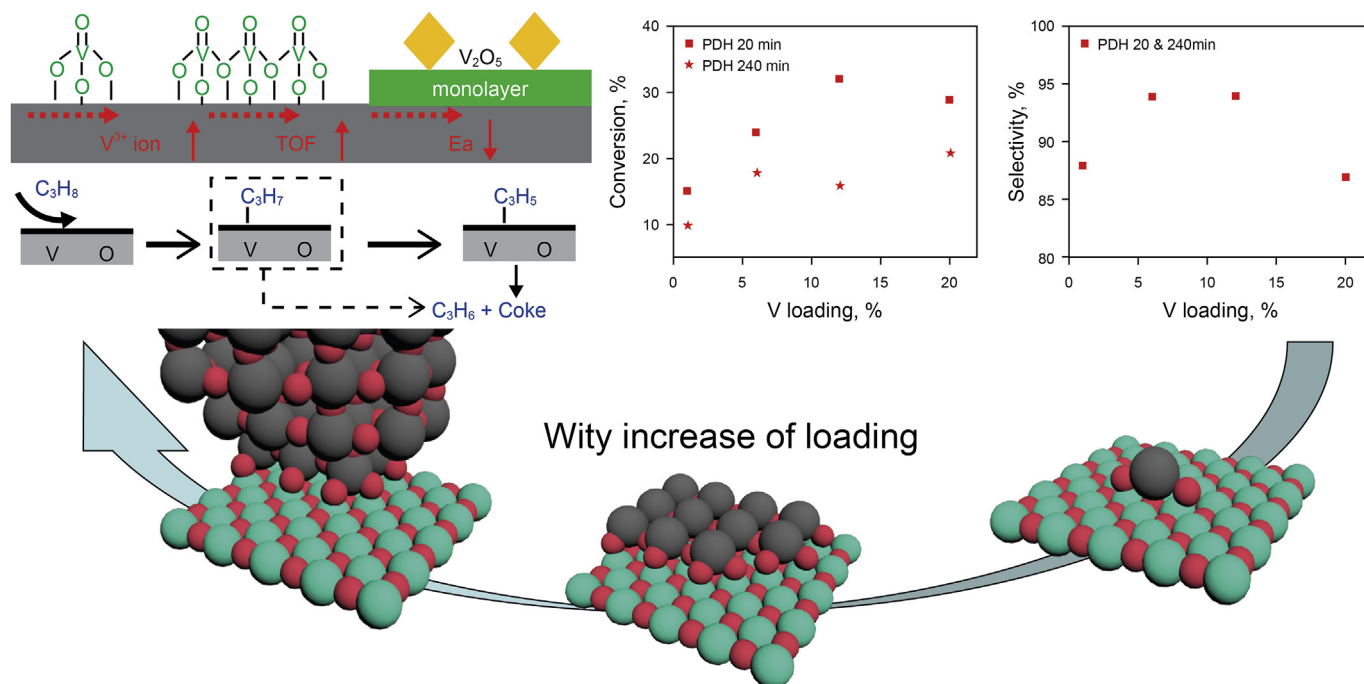


Fig. 6. Change of surface structure of the oxide active sites and catalytic performance by different loading (Liu et al., 2016).

temperature due to physical wrapping effect. In addition, the electron interaction between CN materials and ZnO also promoted the desorption of propylene. This ZnO catalyst has excellent conversion, selectivity and stability.

Evolution surface structure of oxide with the change of loading would also be largely determined by type of support, although some inert supports have large specific surface area, they could not disperse the active components well. Santhoshkumar et al. (2009) found Cr is more likely to exist as isolated Cr (VI) species under low loading on the SBA-15. These isolated sites have highly activity and stability. However, with the increase of the loading amount, α -Cr₂O₃ gradually formed from isolated Cr species and result in a decrease of activity. On the contrary, although in the low loading Cr exists as oligomers on the Al₂O₃ with relatively low activity, α -Cr₂O₃ oxide does not appear even in a high loading. Therefore, CrO_x/Al₂O₃ have higher conversion than CrO_x/SBA-15 in high loading. Rossi et al. (1992) studied the catalytic activity and texture properties of CrO_x species on SiO₂, Al₂O₃ and ZrO₂. The result of PDH show CrO_x supported on ZrO₂ has a much higher activity due to the highly dispersed chromium species, this may be due ZrO₂ has higher ability to disperse chromium catalyst as isolated sites. Supports also could affect coordination environment of active metals through M-O-S bonds (M is the active metal center, S is the support), and result in influence on the reducibility of supported oxide. Xie et al. (2020) found ZrO₂ can effectively improve the TOF of VO_x than the sample using Al₂O₃ as support. The VO_x/ZrO₂ catalysts shows more loss of coordination oxygen atoms than VO_x/Al₂O₃, and activity of lower coordinated V-O pair on ZrO₂ shows six times higher than Al₂O₃. Author also measured reducibility of V-O-V dimer on Al₂O₃ and ZrO₂ though a DFT calculation, result showed V-O-S and V-O-V bond in VO_x/ZrO₂ are weaker than VO_x/Al₂O₃.

In the isolated active sites, metal-oxygen active pairs are closely connected with the support through M-O-S bonds, their catalytic performance are more greatly affected by the support. Organic precursor directed synthesis make M-O-S interaction in well-defined oxide catalysts possible. Szeto et al. (2018) synthesized

well-defined isolated Ga catalysts supported respectively on Al₂O₃ and SiO₂ by SOMC method, which Ga species exist as isolated single-atoms on Al₂O₃ and double-atom on SiO₂. Ga₁/Al₂O₃ appears to show more active and selective catalyst than Ga₂/SiO₂. This may be due to Ga-O-Al sites have higher C-H cleaver activity than Ga-O-Si, thus proved the importance of support in oxide catalysts. This strong interaction between oxide and support decide isolated sites sometimes may not be the best active site, for example, strong support-oxide interaction would cause isolated oxide sites difficult to be reduced into coordination unsaturation state, and thus resulting in low activity. Liu et al. (2016) found isolated VO_x has lower TOF than V₂O₅ crystalline in VO_x/Al₂O₃. The lower reducibility of V-O-Al bond than V-O-V bond may be the reason of their poor activity, which result in most vanadium species are only reduced to V⁴⁺ instead of highly active V³⁺. The M-O-S bonds sometimes lead to the formation of B-acid sites which would catalyzes side reactions (Castro-Fernández et al., 2021). Therefore, compatibility of isolated oxide catalysts should be carefully considered according to the types of supports.

In some bulk catalysts such as ZrO₂ (Zhang et al., 2018), TiO₂ (Li et al., 2020), Al₂O₃ (Wang et al., 2020), Ga₂O₃ (Zheng et al., 2005), particle size, crystal phase and degree of surface defects would play a similar role instead of dispersion. For Zr-based catalysts, oxygen vacancies on zirconia surface are widely considered as the source of activity. (Otroshchenko et al., 2015). Zhang et al. (2018) found that ZrO₂ monoclinic crystal with smaller particle size shows higher intrinsic activity than bigger one. The effect is more obvious when the particle size is below 10 nm. This is due to more amount of surface defects such as corner, edge exist on the small ZrO₂ crystal and results a higher oxygen vacancy concentration. At the same time, coking selectivity would decrease with the decrease of ZrO₂ crystal size, this may be due to small nanoparticle have more dispersed active sites. Zhang et al. (2019a,b) also studied the effect of crystal phase of ZrO₂ on catalytic performance. Decreasing of particle size would increase activity of ZrO₂ in either monoclinic phase or tetragonal phase. However, although they have similar activation energy, monoclinic ZrO₂s have a higher conversion than

tetragonal ZrO_2 . This phenomenon can be explained by that lattice oxygen in monoclinic ZrO_2 has a better mobility than that on tetragonal ZrO_2 . Zheng et al. (2005) tested catalytic performance of various Ga oxide with different morphology. Catalytic activity tests found $\beta\text{-Ga}_2\text{O}_3$ has the highest specific activity of PDH in different polymorphs of Ga_2O_3 . NMR and NH_3 adsorption indicated that $\beta\text{-Ga}_2\text{O}_3$ has higher Lewis acid sites and tetra Ga^{3+} density than other polymorphs of Ga_2O_3 , this shows that the Lewis acid sites is closely related to the tetra coordinated Ga^{3+} and these Lewis acid sites are related with activity strongly.

4.3. The role of promoter

For oxide catalysts, adding appropriate promoters could effectively change the geometry and electronic structure of the active sites, thus affecting the performance of the catalysts (Sattler et al., 2014). Interaction between promoters and active oxide could be classed to two interaction: oxide-oxide and metal-oxide interaction. This interaction depends on the existing form of promoter. For oxide-oxide interaction, heteroatom would effectively change redox properties or affects the acidity and basicity of oxide surface, thus effectively effect catalytic performance (Ruiz Puigdollers et al., 2017). However, due to complexity of oxide catalysts, systematic researches on predicting what kind of element would in oxide catalysts is still difficult. From the experience, oxyphilic or basic elements often lead to lower activity but higher stability, while the dopants with acid elements (most of them could be used as independent active components) are conducive to the improvement of dehydrogenation activity (Liu et al., 2020; Li et al., 2016; Zhang et al., 2019). Oxide-oxide interaction could also affect the aggregation morphology of active oxides through M-O-M bonds and thus affecting the dispersion of active sites. For metal-oxide interaction, metals especially noble metals could activate hydrogen molecules into high energy hydrogen atoms, so they could introduce hydrogen spillover or reverse spillover effect to adjust the reducibility of oxide or part in hydrogen evolution step in PDH (Otroschenko et al., 2015; Sattler et al., 2014). The metal-oxide interface could also affect geometry and electronic structure of the active sites in some case (Liu et al., 2016).

Doping metal element could be achieved by simple co-impregnation or sequential impregnation method and effectively effect catalytic performance, thus they have been widely studied. Alkali metals such as Na and K are the most common metal promoters used in PDH. They could poison strong acid sites on surface of catalysts, which are considered to prone catalyzing side reactions such as coking. In addition, the addition of K is also conducive to improve dispersion of the oxide species on the support (Sattler et al., 2014). Other elements, such as Ce (Zhang et al., 2019), Zn (Liu et al., 2020), Ni (Li et al., 2016), have also been used in Cr-based catalysts as promoters. Zhang et al. (2019) studied the role of Ce in $\text{CrO}_x/\text{Al}_2\text{O}_3$ catalyst. The interaction between Ce and Cr results in more oxygen vacancies and after modification of Ce. Addition of Ce effectively reduced the inactive Cr^{6+} species and the dispersion of CrO_x species, thus stability, selectivity and conversion are effectively improved. Wu et al. (2017) explained in detail the structure-reaction relationship of Mg promoter in $\text{VO}_x/\text{Al}_2\text{O}_3$. The addition of Mg would disperse V_2O_5 crystals (which is mainly contributors of coke) into oligomeric or isolated VO_x structure (Fig. 7c). This effect not only effectively decrease quantity of coke, but also results in a better conversion due to higher dispersion. However, excessive addition of Mg oxide would form MgO aggregation and cover active VO_x , which lead to decline of activity. Precious metals are used as promoters. Liu et al. (2016) prepared a novel $\text{ZnO}/\text{Al}_2\text{O}_3$ catalyst doped by trace amount (0.1 wt%) of platinum for PDH. Comparing to traditional ZnO catalyst, the addition of trace amount platinum

greatly improves the reduction resistance of zinc oxide and reduces the formation of unstable metallic Zn. In addition, Pt improves the desorption of H_2 and C–H activation on the surface of Zn oxide. Further characterization indicate that Pt clusters are highly dispersed and covered by ZnO. Authors indicate these Pt clusters would increase the Lewis acidity of zinc through electronic interaction and promotes the desorption of adsorbed hydrogen atoms, this effect could reduce overreduction of unstable metallic Zn and increase ZnO activity (Fig. 7b). Sn supported by SiO_2 catalyst recently has high selectivity and activity, but at high temperature, the reduced Sn will aggregate and lead to the decrease of activity (Wang et al., 2016; Wang et al., 2020; Liu et al., 2020). Wang et al. (2016) found that after adding a small amount (0.05 wt%) of Pd into Sn/SiO_2 would effectively increase stability of catalysts, the life of Sn catalyst was prolonged by more than two times. Authors found introduction of Pd could decrease aggregate degree of Sn species and reduce the loss of tin at high temperature, thus improve activity and stability.

Except for metal elements, some non-metallic oxides such as SO_x , PO_x can effectively improve the negative electron properties of oxide. Sun et al. (2014) found that the introduction of SO_4^{2-} into Fe_2O_3 could effectively improve the yield of propylene and stability. This better catalytic performance may be due to the presence of SO_4^{2-} also lead to electron deficiency of Fe atoms, which makes absorb negatively charged second carbon of propane easier and provide a higher activity. In addition, promoting sulfur could also stabilize Fe chemical state and the inhibiting formation of harmful species, such as FeC_x or FeS (Sun et al. 2014, 2015). Tan et al. (2016) synthesized a serious phosphorus containing $\text{Fe}/\text{Al}_2\text{O}_3$ catalysts. The addition of phosphorus plays an important role in creating more active sites, while the Fe_2O_3 without phosphorus will coked severely and have a low selectivity. After adding phosphorus, the catalyst with best performance has a conversion about 14% and a selectivity of 80%. In addition, longer duration experiment indicated that the conversion and selectivity of catalyst can be almost unchanged in 24 h. Gu et al. (2020) modified vanadium oxide surface supported by Al_2O_3 with phosphorus by gas phase reduction method. After proper modification, the activity of the catalyst decreased slightly, but the stability increased greatly. This may be due to P dispersing VO_x polymerization to isolated V sites, which have lower activity but higher stability. The addition of phosphorus also reduces the acidity of the oxide, thus improving the overall stability of the catalyst.

While further improving second metal loading, dopant would increase in diffusion probability and react with the original oxide to bimetallic compound structure or solid solution. Formation of stable bimetallic oxides often leads to decreasing number of active sites and poor catalytic performance. But sometimes the formation of new structures is also conducive to the formation of better active sites than supported oxide. Chen et al. (2008) synthesized a kind of $\text{Ga}_2\text{O}_3\text{-Al}_2\text{O}_3$ solid solution catalyst with a spinel structure. Compared with the traditional $\text{Ga}_2\text{O}_3/\text{Al}_2\text{O}_3$ catalyst, the formation of solid solution can effectively disperse and stabilize the gallium oxide species. Although $\text{Ga}_2\text{O}_3\text{-Al}_2\text{O}_3$ solid solution has a slight decreasing in the initial conversion rate compare to $\text{Ga}_2\text{O}_3/\text{Al}_2\text{O}_3$, it has more stable catalytic performance, this enhancement effect is shown in Fig. 7d. Otroschenko et al. (2017) studied the promoting role of Cr in CrZrO_x bimetallic bulk oxide. The addition of Cr promotes the lattice oxygen removal by activate H_2 molecule to active hydrogen atom and thus improve coordinatively unsaturated Zr^{4+} sites formation, which has high dehydrogenation activity. Therefore, CrZrO_x has higher activity than pure ZrO_2 catalysts and even industrial $\text{CrO}_x/\text{Al}_2\text{O}_3$ catalysts. In addition, lattice CrO_x species are also responsible to reduce the strength and amount of strong acid sites on ZrO_2 , which reduce side reaction caused by Lewis acid sites.

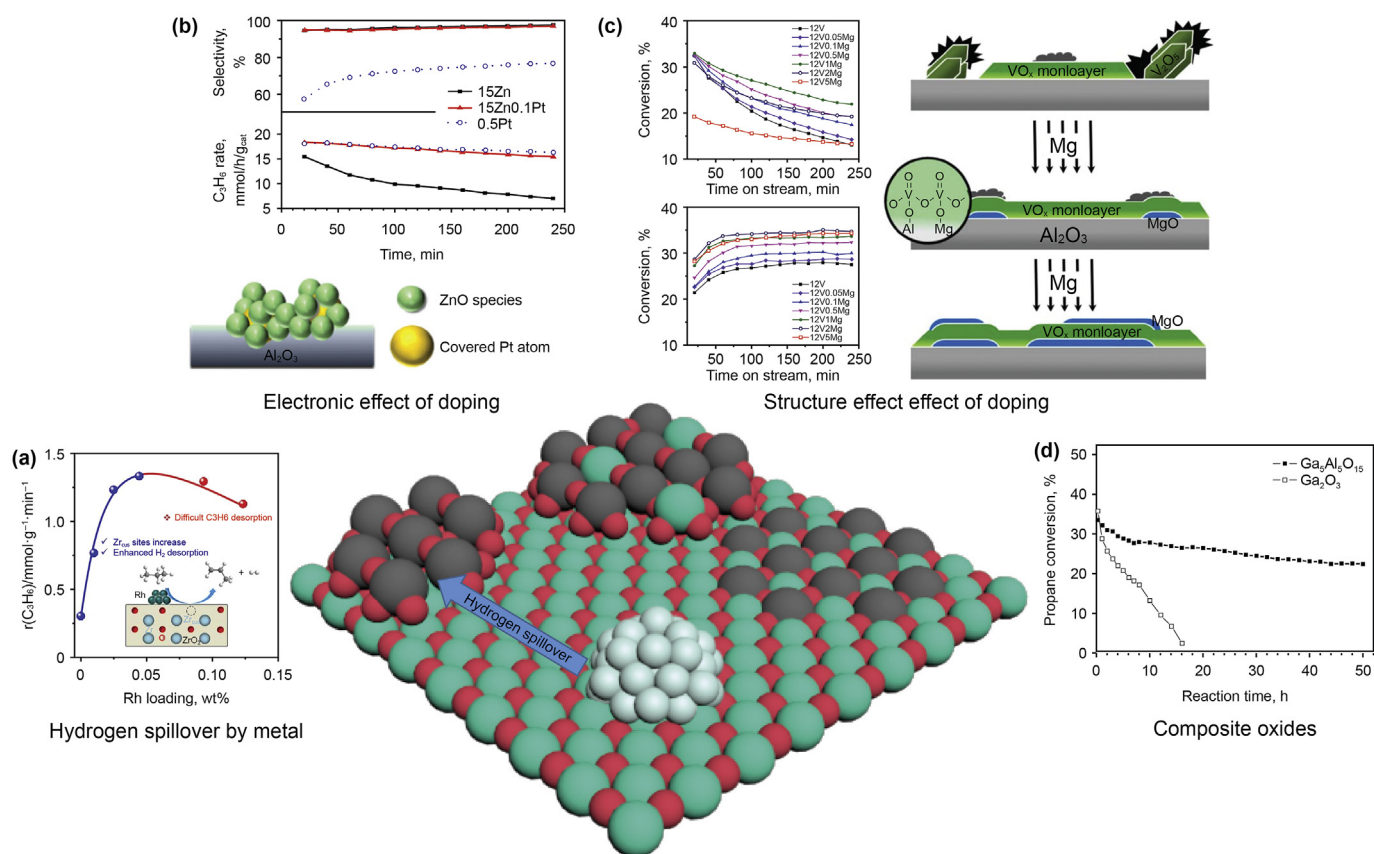


Fig. 7. (a) Rhodium improves the density of active sites on zirconia surface through hydrogen spillover effect (Zhang et al., 2020) (b) Doping platinum in ZnO catalyst can effectively improve Lewis acidity and thus obtain higher activity (Liu et al., 2016) (c) The surface structure of vanadium oxide changes with increasing doping of Mg (Wu et al., 2017) (d) Comparison of gallium oxide, alumina solid solution and pure gallium oxide (Chen et al., 2008).

Compared with the supported $CrO_x/LaZrO_x$ catalysts, the bimetallic $CrZrO_x$ oxide catalyst has better regeneration stability and activity at the same acidity number.

Metals especially noble metals could also play a role of promoter by introducing hydrogen spillover effect, this effect could recombine adsorbed hydrogen atoms or adjust the reducibility of oxide catalysts. Sattler et al. (2014) synthesized a Pt– Ga_2O_3/Al_2O_3 with trace platinum content of only 0.001 wt%. Although both platinum and gallium oxide are considered to have catalytic activity in some previous studies, this catalyst has better conversion and selectivity than one of them exist alone. It is assumed that promoting role of Pt is accelerating recombination of the hydrogen atoms to H_2 which is reverse reaction of hydrogen spillover. The stability and size of Pt particles would greatly affect the hydrogen spillover effect. Han et al. (2019) studied the promoting effect of Cr in a series of supported $CrZrO_x$ catalysts. They found Cr atoms would activate H_2 molecule to active hydrogen atom and promote coordinatively unsaturated Zr^{4+} sites formation, which has high dehydrogenation activity. This synergy effect could effectively reduce the usage of toxic Cr and expensive Zr but keep the activity unchanged.

Promoter has a similar effect to improve catalytic properties of bulk oxide. Otroshchenko et al. (2017) studied the influence of doping Li, Ca, Mg, Sm, La in $MZrO_x$ catalysts (M stands for dopant). Doping of ZrO_2 with Ca or Li would result a low activity. On the contrary, Addition of La, Sm, Y would effectively enhance propylene formation rate of ZrO_2 . Creation of more surface defects on ZrO_2 after adding heteroatoms may be the cause of these activity changes. Noble metals such as Pt, Rh, Ir and some hydrogen-activated metals such as Cu could provide hydrogen spillover

effect, which improve reducibility and amounts of active sites (Otroshchenko et al., 2015). Zhang et al. (2020) carried out a more systematic study interaction between ZrO_2 and Rh nanoparticles in Rh/ ZrO_2 catalyst. Experiment and calculation results indicated the addition of Rh increase the oxygen vacancy number on the surface of ZrO_2 which is widely considered to main active sites, thus effectively improve conversion. However, excessive addition of Rh would lead to a decrease in activity, this may be due to too many oxygen vacancies would restrain the desorption of C_3H_6 and hindered PDH reaction (Fig. 7a). Recent oxide catalysts are shown in Table 2.

5. Coke deposition in PDH

5.1. Mechanism of coke deposition

Coke is the general term of deep dehydrogenation alkyls or graphitized carbon deposition (Sattler et al., 2014). In PDH, coke deposition path mainly includes four steps: deep dehydrogenation, C–C bonds breaking, formation of aromatic hydrocarbon and graphitization (Huš et al., 2020; Lian et al., 2018; Zhao et al., 2015). But actually, its detail mechanism and key intermediates is still ambiguous until now. Researchers have proposed some possible processes in deep dehydrogenation process basis on DFT. Valcárcel et al. (2006) studied stability of a variety of intermediates of deep dehydrogenation on Pt (111) include 1-propenyl, propylidyne, propenylidene, and propyne. Among these intermediates, propylidyne has the lowest energy and preferentially adsorb on hollow of three platinum atoms. This work pointed out the most stable

Table 2
Catalytic performance of metal oxide catalysts.

Catalysts	Feeding composition	Reaction temperature, °C	Space velocity, h ⁻¹	flow rate, ml/min	Conversion, %	Selectivity, %	Test time, h	Size of catalysts, mesh	catalysts loading, g	Ref
1V/ZrO ₂	Propane:nitrogen:hydrogen = 7:36:7	550	/	50	24.7	82.2	/	20–40	0.4	Xie et al. (2020)
1.97Ga/Al ₂ O ₃	Propane:argon = 1:4	550	/	5	23.1–10.2	78–85.2	24	/	0.08	Szeto et al. (2018)
5Co–Al ₂ O ₃ sheets	Propane:hydrogen:nitrogen = 1:0.8:3.2	590	2.9	/	23.3	97.2	5	30–60	0.15	Dai et al. (2020)
5Cr–5Ce/Al ₂ O ₃	Propane:nitrogen = 14:86	630	/	29	42.7	76.6–55.2	3	60–80	0.4	Zhang et al. (2019)
12V1Mg/Al ₂ O ₃	Propane:hydrogen:nitrogen = 7:7:11	600	3	/	32.8–23.2	83.4–91.2	4	20–40	0.25	Wu et al. (2017)
10V0.1K/meso-Al ₂ O ₃	1:4 = nitrogen:propane	610	/	30	59.6–17.3	~85	10	20–60	1	Bai et al. (2016)
15Fe4P/Al ₂ O ₃	Hydrogen:propane = 1:19	600	/	10	17	75	6	/	0.2	Tan et al. (2016)
2.5Zn@NC/S-1	Hydrogen:propane:nitrogen = 1:1:5	600	/	17.5	56.1–48	85–89.7	5	40–60	0.2	Zhao et al. (2019)
Ga ₂ O ₃ –Al ₂ O ₃	1:39 = propane:nitrogen	500	/	10	38–23	92.3–98	8	/	0.2	Chen et al. (2008)
0.1Pt15Zn/Al ₂ O ₃	Propane:hydrogen:nitrogen = 1:1:8	600	3	50	34.3–32.5	93.6–97.3	4	20–40	0.5	(Liu et al., 2016)
0.1Pt3Ga/Ce–Al ₂ O ₃	Propane:helium = 1:4	620	5.4	/	56.6–51.2	~98	1	75–100	/	Im et al. (2016)
1Sn-DMSNs	Pure propane	600	/	8	17.6	87.2	8.5	40–80	0.3	(Liu et al., 2020)

hydrocarbon intermediate in PDH on Pt (111) surface. In another DFT calculation of Yang et al. (2010), they indicated with the process of dehydrogenation the energy barrier of C–C scissor decreases continuously. Propyne was found to be the most likely starting point for C–C scissor to coke deposits. Many other studies have obtained similar conclusion (Saerens et al., 2017). In addition to coking directly caused by active sites, acidic sites also catalyze the coking process, Lewis or Bronsted acid sites would catalyze coke formation like a catalyzed aromatic hydrocarbon process and follow an acid-catalyzed carbocation mechanism (Sattler et al., 2014).

Although the mechanism of coke deposition is still uncertain, C₁ and C₂ species are generally considered as main precursor of coke deposition rather than C₃. These species have more lone electrons and would attract each other and form aromatic rings through surface-mediated mechanism. (Larsson et al., 1996; Lian et al., 2018; Saerens et al., 2017). Jackson et al. (1997) proved polycyclic aromatics formed on Pt/Al₂O₃ in PDH are more likely derived from C₁ species rather than C₃ species used a mathematical derivation. After detecting coke by mass spectrometry, they found main component of coke are pyrene and methyl pyrene and they cannot be divided by three. In addition, isotopic labeling experiments also proved C₃ species would be divided into C₁ in the process of coke deposition. Up to now, most of the DFT experiments use the polymerization of C₁ or C₂ to aromatic ring as the main carbon deposition process. (Lian et al., 2018; Saerens et al., 2017). After the formation of the first aromatic ring, the aromatic ring precursor expands continuously to polycyclic aromatic hydrocarbons through a Diels–Alder mechanism, finally form highly graphitized coke.

For either metal catalysts or oxide catalysts, coke deposition are the main culprit of deactivation. In industrial process, Pt-based catalysts need to be regenerated every 7–8 h. For Cr-based catalyst, this regeneration would be more frequent and one-way reaction time is only about 10 min (Sattler et al., 2014). Although sometimes coke also show some advantages in Cr-based catalysts, such as they could provide additional energy in burning regeneration step. But for platinum-based catalysts, heat from combusting coke would lead to serious sintering even more serious than

reaction step (Kaylor and Davis, 2018). In order to understanding effect of coke deposition, researches on coke deposition in PDH could be described from three levels: macro-levels, meso-levels and micro-levels (Ye et al., 2019). In view of macro-level, coke will influent mass and heat transfer process, its influence is closely related to type of reactor and the reaction technology. Limitation of research focus of this paper, we would ignore detailed discussion for this influence. Recently, understanding and inhibiting coke deposition at a meso- and micro-level has attracted a lot of attention.

5.2. Mesoscopic effect of coke and pore structure

In view of meso-level, coke product would narrow and finally block pore channels, causes diffusion resistance and leads to deactivation (Ye et al., 2019). Proper pore structure could improve carbon capacity and thus reduce block effect. In addition, pore structure could play an important role in diffusion of propylene, and thus shorten the contact time between propylene and active sites to reduce coke deposition. Ye et al. (2019) built a pore network model of PtSn/Al₂O₃ and use it to simulated its coke deposition process. According to the simulation results, increasing of pore connectivity and volume-averaged pore radius did not obviously influence the coke formation rate, but increased the maximum coke deposition. Decrease of pore size distribution would not affect the rate of coke deposition, but significantly increase maximum coke capacity. In addition to pore structure, the pore radius can't make a great impact on carbon capacity but is proportional to the rate of coke deposition. Ye et al. also simulated the in-situ change of pore structure in deactivation process. Due to obvious diffusion limitation, in the first stage, propylene is difficult to diffuse from the inside to outside and thus coke form mainly in the nearly center part of catalyst, catalysts would suffer a rapid deactivation step. In the second stage, the pores in the center are almost blocked, so coke mainly exists in the outer region of the particles and the rate of coke deposition slows down.

How to control the appropriate pore structure to minimize coke deposition has attracted extensive attention of researchers. Straight

uniform pore is widely considered to be more favorable for propane dehydrogenation. Accumulation of particles could form some natural pores, but these inter-crystalline pores usually don't possess uniform size and have many structural defects such as curved and closed structures, which are not conducive to mass transfer. In industrial, shaping catalysts with high pressure is needed to homogenize size of channel of supports, this usually requires an ultra-high pressure of more than 100 MPa. Therefore, some monolith materials such as ordered mesoporous oxide, molecular sieve which has uniform and natural pore structure have attracted largely attention. Creation of ordered multistage pores also plays an important role in promoting mass transfer. Li et al., 2017 prepared a series of PtSn/TS-1 catalysts with different particle sizes by hydrothermal synthesis. Although TS-1 is a microporous molecule sieve, with the decrease of particle size, mesopores gradually appear on surface of TS-1 and the hierarchically porous structure is formed. Compared with TS-1 with large particles, TS-1 with small particles has apparent advantages in conversion, selectivity and stability. The diffusion of products and reactants may be the key to explain this phenomenon. Calculation of Weisz–Prater criterion indicated the PtSn/TS-1 of large particles is seriously affected by internal diffusion but small one has a low resistance to inter-crystalline diffusion. The hierarchically pore structure doesn't only significantly accelerate the diffusion of propylene, but also accelerating the diffusion of propane and avoiding the internal diffusion control. Liu et al. (2020) embedded tin into dendritic mesoporous SiO₂ nanoparticles for PDH. Dendritic mesoporous SiO₂ nanoparticles have mesoporous structure and radial 3D pore with highly connectivity. Changing the ratio of template could regulate the pore structure with different pore size and connectivity, an appropriate pore structure could improve the reaction rate and selectivity.

Dynamic radius of propane (4.3 Å) and propylene are both relatively small, which reduces researchers' attention to the influence of pore structure. Because PDH is one-step reaction, the role of diffusion effect in PDH is often ignored. However, due main and side reactions of propane dehydrogenation is series reaction, the pore structure plays an important role in the selectivity of propane dehydrogenation. At present, most researches on the process of coke deposition focus on the microscopic reaction mechanism of coke. Next, we will discuss the micro-process of coke deposition in detail.

5.3. Micro effect of coke and migration

At a micro scale, coke and coke precursors are rich in lone electrons or electron-rich π bond, active sites would adsorb them strongly and thus result in deactivation. Therefore, those highly unsaturated coordination sites or electrophilic acidic sites are easier to be poisoned by coke. For example, step, edge sites on Pt nanoparticle and over reduced oxide sites are more prone to tightly adsorb C atom and suffered by deactivation (Zhu et al., 2015). Coke would first generate and cover these sites tightly, and thus lead to decrease of conversion. Unsaturated sites are also the main sites which are prone to catalyze cracking and other side reactions, thus coke deposition process is always accompanied by the increase of catalyst selectivity (Gorrioz et al., 1992; Larsson et al., 1996). However, even for terrace of Pt, coke deposition has also been proved to improve selectivity. Lian et al. (2018) explained effect like double-edged sword of coke through a DFT-based kinetic Monte Carlo simulation on Pt (111) in PDH. At the beginning, although conversion in Pt-based catalysts is very high, but the main reaction is deep dehydrogenation rather than formation of propylene. As carbon deposits cover the surface, Consumption rate of propane decreases rapidly, and accompanied by a sharp increase in selectivity.

Snapshots indicated the formation of coke covered and separated the Pt ensembles like alloying promoters such as Sn, and thus increase selectivity.

Reducing coke deposition from both structural and electronic aspects has been widely used in PDH process. Isolated active sites are beneficial to reduce the contact between coke precursors and is helpful to reduce structural-sensitive coke deposition reactions. For metal catalysts, alloying metals as promoter could separate active metal ensembles and deep dehydrogenation species are difficult to form stable transition state on these small ensembles. Isolated catalysts such as SAACs have lower tendency to produce coke (Sun et al., 2018). Electronic effect also plays an important role in inhibiting coke deposition. The promoting metal could transfer the electron to active metal as an electron donor, the electron-rich active sites would exclude the same electron rich π orbitals of propylene and avoid strong adsorption or deep dehydrogenation (Wang et al., 2018). Yang et al. (2012) found Pt alloyed with Sn could effectively broaden d-bandwidth and lead to a downshift of d-center. This downshift of the center of d-band would lead to a higher dehydrogenation barrier, thus Sn slower carbon deposition rate though an electron effect. It should be noticed SMSI can also transfer electron to active sites similar to promoters and thus reduce the deep dehydrogenation reaction (Jiang et al., 2014). In the oxide, the highly isolated active sites are also proved to be beneficial to reduce the formation of carbon deposition, because hydrocarbon precursors adsorbed on these sites are hard to combine with each other and form aromatic rings (Zhao et al., 2019). In addition, the addition of basic promoters could modify affinity of the active site to electron, thus inhibiting coke deposition.

In PDH, precursor of coke and formed coke deposition attached to active sites loosely would be constantly moving on active surface and even move to support surface derived by high temperature, which is also called a self-cleaning effect. This effect is confirmed in two different peaks of temperature programmed oxidation (TPO) experiments of spent catalysts, which showed coke may move into surface of support and further are dehydrogenated to more graphitized coke with higher combusted temperature (Jiang et al., 2014; Redekop et al., 2016; Wang et al., 2018). Some researchers also attribute two kinds of combustion peak to some coke would migrate to far distance from platinum, which could lead oxygen overflow effect of platinum need to a higher energy barrier (Larsson et al., 1996; Redekop et al., 2016). Rich electron density would weaken interaction between coke precursor and active sites thus improve this self-cleaning effect (Iglesias-Juez et al., 2010). Although the amount of coke deposited on Pt–Sn catalysts are even more than on pure Pt catalysts in similar condition, Pt–Sn catalyst still has higher stability. At the same time, the movement of coke is greatly affected by size of platinum particles. Peng et al. (2012) observed by a high-resolution TEM, binding graphene layers will slough off from platinum particles to support due to the strain of structure, which is closely dependent on the particle size. Large Pt particles are more likely to form a carbon layer which coated on the surface of platinum particles. Smaller Pt particles would cause a greater tension on the carbon layer and thus coke would be form of carbon nanotubes or sheets, which are easier to desorb from Pt surface. The movement of the carbon layer will also cause the deformation of platinum nanoparticles due to its strong adsorption and result in the change of reaction performance (Wu et al., 2016). Due to the complex structure of carbon materials, how to correctly understand the role of graphite layer coke still needs further study.

In sum, strategies of anti-coke deposition could be started from both mesoscopic and micro perspectives. On the meso-scale, coking deactivation are mainly caused by channel block, increasing pore size could effectively reduce this process. In

addition, proper pore structure is also important for reducing coke reaction. Straight, uniform and ordered channels are benefit to reduce the residence time of propylene inside catalyst, thus reducing coke deposition. On the micro-scale, deactivation of catalysts mainly comes from the covering of active sites by coke deposition. Isolated active sites are beneficial to inhibit the structure sensitive coke deposition process. From the view of electronic effect, the active sites rich in electrons can weaken the adsorption of coke precursors on the catalyst surface, thus inhibiting the deactivation of coke deposition. These structural and electronic effects could be achieved by adjusting promoters and supports reasonably.

6. Co-feeding gas in PDH

Co-feeding gas in PDH get more and more attention. Traditional feeding gas in PDH is pure propane, sometimes, in order to reduce coke deposition, a mixture of propane and hydrogen is also used in some cases (Saerens et al., 2017). In industrial process, hydrogen would promote reverse reaction of deep dehydrogenation and thus inhibit coke formation, but it also inhibits propane dehydrogenation at the same time. Steam is another widely used co-feeding gas, it could eliminate coke though a water-gas conversion process and reduce the partial pressure of reaction gas. Some mild oxides such as N_2O , CO_2 (Xie et al., 2019) are also used in propane dehydrogenation to improve conversion and reduce coke deposition. But strictly speaking, these are the category of oxidative dehydrogenation after addition these gases. Besides participating in the reaction, these gases also have important influence on the active site structure on the catalyst. How to understand their effect on the reaction is very important to optimizing technology.

Hydrogen is the most important co-feed gas of PDH process in serious industrial Technology. In general, the role of H_2 is considered to promote the deep dehydrogenation and dehydrogenation reverse reaction, and thus reduce the conversion and improve the stability. It should be noted that although hydrogen could participate in the reverse reaction of deep dehydrogenation, it could not reduce has graphitized carbon deposits, which also proves the irreversibility of graphitized coke deposits (Larsson et al. 1996; Redekop et al., 2016). DFT calculations and experiments also has proved hydrogen adsorbed on the surface would also promote the desorption of propylene and increase the energy barrier of dehydrogenation, thus inhibit further dehydrogenation of propylene to coke deposition. Sattler et al. (2013) found addition of H_2 not only reduces the total amount of coke deposition, but also effect the structure of coke deposit. Though the analysis of Raman spectrum and TGA, researcher observed the coke deposit has a smaller size and a more graphitized structure after adding hydrogen. This finding also verifies DFT's conclusion. In fact, sometimes the addition of hydrogen will lead to the improvement of both stability and conversion, this anti-common phenomenon is considered to be related to adsorption effect. Saerens et al. (2017) tested influence mechanisms of hydrogen in Pt-based catalysts on the activity of PDH though a microreactor simulation. In addition to increasing the dehydrogenation barrier, highly partial pressure of hydrogen in feedback gas would not only reduce deep dehydrogenation species but also free active sites. Thus, appropriate addition of H_2 would create more free sites on the surface and increase in activity. On the oxide, the addition of hydrogen could also change the properties of active sites, resulting in the change of reaction performance (Zhao et al., 2018). Therefore for different types of catalysts, hydrogen atoms could not only participate in surface reactions, but also change the structure of active components, the role of hydrogen should be carefully considered due to different hydrogen absorption ability.

Steam is a good choose of feeding gas in industrial process which can reduce the partial pressure of propane, promote the reaction equilibrium moving forward and at the same time can be used as a good heat conducting material. Though a reaction similar to water gas conversion, steam can reduce the rate of coke deposition. However, in high temperature, co-feeding steam will accumulate in breaking of structure of supporters, such as Al_2O_3 , zeolite, basic metals are commonly used in improving stability of these materials. In some oxide catalysts, such as zirconia, the addition of steam would cover the active sites and completely inactivate the catalyst (Otroschenko et al., 2017). In some systems, the chemical reaction of water vapor with active component also plays a positive role. Shan et al. (2015) found the addition of steam would change alloying structure of Pt–Sn catalyst. After proper steam pretreatment time, the size of platinum particles will decrease and thus improve activity. Promotion of steam would oxidize the Sn(0) component to SnO_x , resulting in the partly dealloying of Pt–Sn catalysts and formation of highly active alloying components Pt_3Sn , thus decrease dehydrogenation barrier. As a cheap additive, steam has high research value.

7. Summary and prospect

Today, uncertain volatility of oil price, decreasing crude oil resource, energy consumption and carbon emission are driving traditional petrochemical industry to reexamine the utilization efficiency of carbon atoms. Utilization of propane is a very challenging but promising part in petrochemistry, while it traditionally is used as gas fuel with a lot of CO_2 emission. In order to utilize these resources in green way, PDH technology need pay more attention. From the perspective of atomic economy, PDH is a fuel-chemical conversion process with high carbon utilization, in which propylene is its only product. In PDH, hydrogen as a by-product with almost zero pollution, which is an important low-carbon fuel and reaction gas. Traditional hydrogen comes from fossil fuels and is accompanied by a large amount of CO_2 emissions. Undoubtedly, widening propane dehydrogenation process will provide a “ $1 + 1 > 2$ ” effect in either environment friendliness and economic benefits. However, traditional industry catalysts have their intrinsic shortcoming such as fast coke deposition and high toxicity of Cr-based catalysts and expensive price of Pt-based catalysts. In order to further improve this potential technology, structure-activity relationship of catalysts should be paid a lot of attention.

For metal-based catalysts, it is proved that PDH takes place on adjacent metal atoms from one to multiple. The activity and selectivity of propane dehydrogenation are closely related to coordination environment and continuity of metal atoms. Catalytic performance of metal active sites can be effectively adjusted by forming alloy with second metal, electronic effect and ensemble effect often be used to reveal promoting role of alloy. Traditional support in metal-based catalysts is Al_2O_3 or SiO_2 . Highly dispersed alloy particles could be achieved by precisely adjusting the defect site structure or surface geometry of them. Recently, some semiconductor material such as TiO_2 , CeO_2 were also used as supports due to their electronic effect. We think future research in metal catalysts should focus on the structure of alloys, defect sites engineering of inert supports and interaction between alloy nanoparticles and “active” support. For alloying nanoparticles, different surface alloying structure such as substitutional solid-solution alloys, interstitial solid-solution alloys, intermetallic alloy and amorphous alloy with different alloying elements should be studied separately to detail the role of alloying promoter. The substructure and internal structure of nanoparticle should also be paid enough attention due to their important electronic interaction

with surface atoms. In the aspect of support, the commonly used supports such as alumina and silica have high specific surface area and adjustable hole structure but still need to be further improved their interaction between metal and support. Their morphology and defect sites should be precisely modified to improve dispersion of supported nanoparticle. Considering that most of the traditional supports are electrically inert, those “active” supports which interact with metal nanoparticle though electronic effect provide new possibilities for the further development of metal catalysts. How to make better utilization of their interaction and improve the specific surface area is more important.

For oxide-based catalysts, the active sites of oxides are often considered to be metal-oxygen pairs with unsaturated coordination. Reduction plays an important role in determining the microstructure of active sites include coordination of unsaturated metallic cation, hydroxyl et al. Catalytic mechanisms on oxides catalysts are varied, which are closely related to the properties of metals and oxygen. Oxide could exist as different degree of polymerization on the support, such as isolated sites, polymerized sites or crystalline on the support. Due to the different bonding between the metal center and the support, their catalytic performance is also significantly different. Isolated sites are widely considered as the most favorable active sites for oxides because of their high dispersion and low coke deposition tendency, but considering their strong interaction with support, catalytic performance of isolated sites still needs to be carefully deliberated according to the coordination structure. Oxide catalyst could be further modified by adding metal or oxide promoters. Though metal-oxide interaction or oxide-oxide interaction, promoter would change the degree of polymerization or the electronic structure of active sites. Based on the above analysis, we outline that future development direction of oxide catalysts should focus on deeply understanding the mechanism and interface effect of oxide-oxide and metal-oxide. At present, most of the catalytic mechanism of oxide catalysts come from mechanism of homogeneous C–H activation process catalyzed by metal complexes. However, the mechanism of heterogeneous catalysis is still unclear because detecting evolution of active sites in solid-gas two-phase is much more difficult than single-phase solution. Considering that there are many kinds of oxide catalysts, structure of active sites and reaction mechanism in each of them should be carefully analyzed individually. Metal and oxide promoters play an important role in improving the performance of oxide catalysts. Although many studies have found that a variety of element have positive effects in oxide catalysts, due to complex structure of interface, their promoting mechanism is still unclear. Adjusting their interaction through interface engineering is very promising to not only obtain higher activity but also establish structure-activity relationship between promoter and oxide. Especial the noble metal-oxide interaction, some recent reports even found that noble metals as promoters in oxide can achieve higher catalytic performance than noble metals as active components, regulatory interaction between noble metal and oxide though control the interface need more attention for replacing expensive noble metal catalysts with cheap oxides.

Except for structure-activity relationship dominated by chemical effect, pore structure and mass transfer should be also emphasized. Reasonable design of highly interconnected, uniform pore with appropriate size plays an important role in further improving catalyst performance, especially anti-coking performance. The influence of pore structure should be paid more attention in the synthesis of supports. Influence of co-feeding gases on structure of active sites is also highly concerned in this review. We think future research in co-feeding gas should focus on some alkane-associated gas or gas easy to be separated in order to further improvement of dehydrogenation process.

Acknowledgment

This work was supported by the National Natural Science Foundation of China (21872163, 21972166), National Engineering Laboratory for Mobile Source Emission Control Technology (NELMS2017A05), Beijing Natural Science Foundation (2202045, 2182060), PetroChina Innovation Foundation (2018D-5007-0505).

References

- Akah, A., Al-Ghrami, M., 2015. Maximizing propylene production via FCC technology. *Applied Petrochemical Research* 5, 377–392. <https://doi.org/10.1007/s13203-015-0104-33>.
- Al-Douri, A., Sengupta, D., El-Halwagi, M., 2017. Shale gas monetization – a review of downstream processing to chemicals and fuels. *J. Nat. Gas Sci. Eng.* 45, 436–455. <https://doi.org/10.1016/j.jngse.2017.05.016>.
- Alabdullah, M.A., Gomez, A.R., Vittenet, J., Bendjeriou-Sedjerari, A., Xu, W., Abba, I.A., et al., 2020. A viewpoint on the refinery of the future: catalyst and process challenges. *ACS Catal.* 10 (15), 8131–8140. <https://pubs.acs.org/doi/10.1021/acscatal.0c02209>.
- Aly, M., Fornero, E.L., Leon-Garzon, A.R., Galvita, V.V., Saeys, M., 2020. Effect of boron promotion on coke formation during propane dehydrogenation over Pt/ γ -Al₂O₃ catalysts. *ACS Catal.* 10 (9), 5208–5216. <https://doi.org/10.1021/acscatal.9b05548>.
- Atanga, M.A., Rezaei, F., Jawad, A., Fitch, M., Rownaghi, A.A., 2018. Oxidative dehydrogenation of propane to propylene with carbon dioxide. *Appl. Catal. B Environ.* 220, 429–445. <https://doi.org/10.1016/j.apcatb.2017.08.052>.
- Bai, P., Ma, Z., Li, T., Tian, Y., Zhang, Z., Zhong, Z., et al., 2016. Relationship between surface chemistry and catalytic performance of mesoporous γ -Al₂O₃ supported VO_x catalyst in catalytic dehydrogenation of propane. *ACS Appl. Mater. Interfaces* 8 (39), 25979–25990. <https://doi.org/10.1021/acsami.6b07779>.
- Bauer, T., Maisel, S., Blaumeiser, D., Vecchiotti, J., Taccardi, N., Wasserscheid, P., 2019. Operando DRIFTS and DFT study of propane dehydrogenation over solid- and liquid-supported Ga_xPt_y catalysts. *ACS Catal.* 9 (4), 2842–2853. <https://doi.org/10.1021/acscatal.8b04578>.
- Belskaya, O.B., Stepanova, L.N., Gulyaeva, T.I., Erenburg, S.B., Trubina, S.V., Kvashnina, K., 2016. Zinc influence on the formation and properties of Pt/Mg(Zn)AlO catalysts synthesized from layered hydroxides. *J. Catal.* 341, 13–23. <https://doi.org/10.1016/j.jcat.2016.06.006>.
- Bhasin, M.M., McCain, J.H., Vora, B.V., Imai, T., Pujadó, P.R., 2001. Dehydrogenation and oxydehydrogenation of paraffins to olefins. *Appl. Catal. Gen.* 221 (1), 397–419. [https://doi.org/10.1016/S0926-860X\(01\)00816-X](https://doi.org/10.1016/S0926-860X(01)00816-X).
- Blay, V., Louis, B., Miravalles, R., Yokoi, T., Peccatiello, K.A., Clough, M., et al., 2017. Engineering zeolites for catalytic cracking to light olefins. *ACS Catal.* 7, 6542–6566. [https://doi.org/10.1016/101442449\(96\)83131-9](https://doi.org/10.1016/101442449(96)83131-9).
- Cai, W., Mu, R., Zha, S., Sun, G., Chen, S., Zhao, Z.J., 2018. Subsurface catalysis-mediated selectivity of dehydrogenation reaction. *Science Advance* 4 (8), r5418. <https://doi.org/10.1126/sciadv.aar5418>.
- Camacho-Bunquin, J., Aich, P., Ferrandon, M., Bean Getsoian, A., Das, U., Dogan, F., 2017. Single-site zinc on silica catalysts for propylene hydrogenation and propane dehydrogenation: synthesis and reactivity evaluation using an integrated atomic layer deposition-catalysis instrument. *J. Catal.* 345, 170–182. <https://doi.org/10.1016/j.jcat.2016.10.017>.
- Castro-Fernández, P., Mance, D., Liu, C., Moroz, I.B., Abdala, P.M., Pidko, E.A., 2021. Propane dehydrogenation on Ga₂O₃-based catalysts: contrasting performance with coordination environment and acidity of surface sites. *ACS Catal.* 11 (2), 907–924. <https://pubs.acs.org/doi/10.1021/acscatal.0c05009>.
- Cesar, L.G., Yang, C., Lu, Z., Ren, Y., Zhang, G., Miller, J.T., 2019. Identification of a Pt₃Co surface intermetallic alloy in Pt–Co propane dehydrogenation catalysts. *ACS Catal.* 9 (6), 5231–5244. <https://doi.org/10.1021/acscatal.9b00549>.
- Chen, M., Xu, J., Su, F., Liu, Y., Cao, Y., He, H., et al., 2008. Dehydrogenation of propane over spinel-type gallia–alumina solid solution catalysts. *J. Catal.* 256 (2), 293–300. <https://doi.org/10.1016/j.jcat.2008.03.021>.
- Chen, S., Pei, C., Sun, G., Zhao, Z., Gong, J., 2020. Nanostructured catalysts toward efficient propane dehydrogenation. *Accounts of Materials Research* 1 (1), 30–40. <https://pubs.acs.org/doi/10.1021/accountsmr.0c00012>.
- Chen, S., Pei, C., Chang, X., Zhao, Z., Mu, R., Xu, Y., Gong, J., 2020. Coverage-dependent behaviors of vanadium oxides for chemical looping oxidative dehydrogenation. *Angew. Chem.* 59, 22072–22079. <https://doi.org/10.1002/anie.202005968>.
- Chen, C., Zhang, S., Wang, Z., Yuan, Z., 2020. Ultrasmall Co confined in the silanols of dealuminated beta zeolite: a highly active and selective catalyst for direct dehydrogenation of propane to propylene. *J. Catal.* 383, 77–87. <https://doi.org/10.1016/j.jcat.2019.12.037>.
- Choi, S., Kim, W., So, J., Moore, J.S., Liu, Y., Dixit, R.S., et al., 2017. Propane dehydrogenation catalyzed by gallosilicate MFI zeolites with perturbed acidity. *J. Catal.* 345, 113–123. <https://doi.org/10.1016/j.jcat.2016.11.017>.
- Conley, M.P., Delley, M.F., Núñez-Zarur, F., Comas-Vives, A., Copéret, C., 2015. Heterolytic activation of C–H bonds on Cr^{III}–O surface sites is a key step in catalytic polymerization of ethylene and dehydrogenation of propane. *Inorg. Chem.* 54 (11), 5065–5078. <https://pubs.acs.org/doi/10.1021/ic502696n>.
- Dai, Y., Gu, J., Tian, S., Wu, Y., Chen, J., Li, F., et al., 2020. γ -Al₂O₃ sheet-stabilized

- isolate Co^{2+} for catalytic propane dehydrogenation. *J. Catal.* 381, 482–492. <https://doi.org/10.1016/j.jcat.2019.11.026>.
- Deng, L., Shishido, T., Teramura, K., Tanaka, T., 2014a. Effect of reduction method on the activity of Pt–Sn/SiO₂ for dehydrogenation of propane. *Catal. Today* 232, 33–39. <https://doi.org/10.1016/j.cattod.2013.10.064>.
- Deng, L., Miura, H., Shishido, T., Hosokawa, S., Teramura, K., Tanaka, T., 2014b. Dehydrogenation of propane over silica-supported platinum-tin catalysts prepared by direct reduction: effects of tin/platinum ratio and reduction temperature. *ChemCatChem* 6 (9), 2680–2691. <https://doi.org/10.1002/cctc.201402306>.
- Deng, L., Miura, H., Shishido, T., Wang, Z., Hosokawa, S., Teramura, K., Tanaka, T., 2018. Elucidating strong metal-support interactions in PtSn and high-energy and its consequences for dehydrogenation of lower alkanes. *J. Catal.* 365, 277–291. <https://doi.org/10.1016/j.jcat.2018.06.028>.
- Dixit, M., Kostetskyy, P., Mpourmpakis, G., StructureVITS, A., Minot, C., 2018. Theoretical study of dehydrogenation- $\gamma\text{-Al}_2\text{O}_3$: site-dependent reactions. *ACS Catal.* 8 (12), 11570–11578. <https://doi.org/10.1021/acscatal.8b03484>.
- Estes, D.P., Siddiqi, G., Allouche, F., Kovtunov, K.V., Safonova, O.V., Trigub, A.L., et al., 2016a. Single-site zinc on silica catalyst surface sites versus molecular analogs. *J. Am. Chem. Soc.* 138 (45), 14987–14997. <https://pubs.acs.org/doi/10.1021/jacs.6b08705>.
- Estes, D.P., Siddiqi, G., Allouche, F., Kovtunov, K.V., Safonova, O.V., Trigub, A.L., et al., 2016b. C–H activation on Co–O sites: isolated surface sites versus molecular analogs. *J. Am. Chem. Soc.* 138 (45), 14987–14997. <https://pubs.acs.org/doi/10.1021/jacs.6b08705>.
- Fan, X., Liu, D., Sun, X., Yu, X., Li, D., Yang, Y., et al., 2020. Mn-doping induced changes in Pt dispersion and Pt_xMn_y alloying extent on Pt/Mn-DMSM catalyst with enhanced propane dehydrogenation stability. *J. Catal.* 389, 450–460. <https://doi.org/10.1016/j.jcat.2020.06.016>.
- Gao, X., Lu, W., Hu, S., Li, W., Lu, A., 2019. Rod-shaped porous alumina-supported Cr₂O₃ catalyst with low acidity for propane dehydrogenation. *Chinese Journal of Catalysis* 40 (2), 184–191. [https://doi.org/10.1016/S18722067\(18\)632024](https://doi.org/10.1016/S18722067(18)632024) (In Chinese).
- Gong, N., Zhao, Z., 2019. Peony-like pentahedral Al_(III)-Enriched alumina nanosheets for the dehydrogenation of propane. *ACS Applied Nano Materials* 2 (9), 5833–5840. <https://doi.org/10.1021/acsnanm.9b01293>.
- Gorri, O.F., Cortes Corberan, V., Fierro, J.L.G., 1992. Propane dehydrogenation and coke formation on chromia-alumina catalysts: effect of reductive pretreatments. *Ind. Eng. Chem. Res.* 31 (12), 2670–2674. <https://doi.org/10.1021/ie00012a007>.
- Gu, Y., Liu, H., Yang, M., Ma, Z., Zhao, L., Xing, W., et al., 2020. Highly stable phosphine modified VO_x/Al₂O₃ catalyst in propane dehydrogenation. *Appl. Catal. B Environ.* 274, 119089. <https://doi.org/10.1016/j.apcatb.2020.119089>.
- Han, Z., Li, S., Jiang, F., Wang, T., Ma, X., Gong, J., 2014. Propane dehydrogenation over Pt–Cu bimetallic catalysts: the nature of coke deposition and the role of copper. *Nanoscale* 6 (17), 10000. <https://doi.org/10.1039/C4NR02143F>.
- Han, S., Zhao, Y., Otroshchenko, T., Zhang, Y., Zhao, D., Lund, H., et al., 2019. Unraveling the origins of the synergy effect between ZrO₂ and CrO_x in supported CrZrO_x for propene formation in nonoxidative propane dehydrogenation. *ACS Catal.* 10 (2), 1575–1590. <https://doi.org/10.1021/acscatal.9b05063>.
- He, Y., Song, Y., Cullen, D.A., Laursen, S., 2018. Selective and stable non-noble-metal intermetallic compound catalyst for the direct dehydrogenation of propane to propylene. *J. Am. Chem. Soc.* 140 (43), 14010–14014. <https://doi.org/10.1021/jacs.8b05060>.
- Hu, B., Schweitzer, N.M., Zhang, G., Kraft, S.J., Childers, D.J., Lanci, M.P., et al., 2015a. Isolated Fe_i on silica as a selective propane dehydrogenation catalyst. *ACS Catal.* 5 (6), 3494–3503. <https://doi.org/10.1021/acscatal.5b00248a>.
- Hu, B., Bean Getsoian, A., Schweitzer, N.M., Das, U., Kim, H., Niklas, J., et al., 2015b. Selective propane dehydrogenation with single-site Co_{II} on SiO₂ by a non-redox mechanism. *Journal of Catalysis* 322, 24–37. <https://doi.org/10.1016/j.jcat.2014.10.018>.
- Hu, P., Lang, W., Yan, X., Chu, L., Guo, Y., 2018. Influence of gelation and calcination temperature on the structure-performance of porous VO_x-SiO₂ solids in non-oxidative propane dehydrogenation. *J. Catal.* 358, 108–117.
- Hu, Z., Yang, D., Wang, Z., Yuan, Z., 2019a. State-of-the-art catalysts for direct dehydrogenation of propane to propylene. *Chin. J. Catal.* 40, 1233–1254. [https://doi.org/10.1016/s1872-2067\(19\)633607](https://doi.org/10.1016/s1872-2067(19)633607) (In Chinese).
- Hu, Z., Ren, J., Yang, D., Wang, Z., Yuan, Z., 2019b. Mesoporous carbons as metal-free catalysts for propane dehydrogenation: effect of the pore structure and surface property. *Chin. J. Catal.* 40 (9), 1385–1394. [https://doi.org/10.1016/s1872-2067\(19\)63334-6](https://doi.org/10.1016/s1872-2067(19)63334-6) (In Chinese).
- Huš, M., Kopač, D., Likozar, B., 2020. Kinetics of non-oxidative propane dehydrogenation on Cr₂O₃ and the nature of catalyst deactivation from first-principles simulations. *J. Catal.* 386, 126–138. <https://doi.org/10.1016/j.jcat.2020.03.037>.
- Iglesias-Juez, A., Beale, A.M., Maaijen, K., Weng, T.C., Glatzel, P., Weckhuysen, B.M., 2010. A combined in situ time-resolved UV–Vis, Raman and high-energy resolution X-ray absorption spectroscopy study on the deactivation behavior of Pt and PtSn propane dehydrogenation catalysts under industrial reaction conditions. *J. Catal.* 276, 268–279. <https://doi.org/10.1016/j.jcat.2010.09.018>.
- Im, J., Choi, M., 2016. Physicochemical stabilization of Pt against sintering for a dehydrogenation catalyst with high activity, selectivity, and durability. *ACS Catal.* 6 (5), 2819–2826. <https://doi.org/10.1021/acs.chemmater.6b00329>.
- Jackson, S.D., Grenfell, J., Matheson, I.M., et al., 1997. Deactivation and regeneration of alkane dehydrogenation catalysts. *Stud. Surf. Sci. Catal.* 111, 167–174. [https://doi.org/10.1016/S01672991\(97\)801528](https://doi.org/10.1016/S01672991(97)801528).
- James, O.O., Mandal, S., Alele, N., Chowdhury, B., Maity, S., 2016. Lower alkanes dehydrogenation: strategies and reaction routes to corresponding alkenes. *Fuel Process. Technol.* 149, 239–255. <https://doi.org/10.1016/j.fuproc.2016.03.006>.
- Ji, Z., Miao, D., Gao, L., Pan, X., Bao, X., 2020. Effect of pH on the catalytic performance of PtSn/B-Zr–O₂ in propane dehydrogenation. *Chin. J. Catal.* 41, 719–729. [https://doi.org/10.1016/s18722067\(19\)63395-4](https://doi.org/10.1016/s18722067(19)63395-4) (In Chinese).
- Jiang, F., Zeng, L., Li, S., Liu, G., Wang, S., Gong, J., 2014. Propane Dehydrogenation over Pt/TiO₂ enhanced performance in propane dehydrogenation. *ACS Catal.* 5 (1), 438–447. <https://doi.org/10.1021/cs501279v>.
- Kaylor, N., Davis, R.J., 2018. Propane dehydrogenation over supported Pt–Sn nanoparticles. *J. Catal.* 367, 181–193. <https://doi.org/10.1016/j.jcat.2018.09.006>.
- Kim, S., Liu, Y., Moore, J.S., Dixit, R.S., Pendergast, J.G., Sholl, D., et al., 2016. Thin hydrogen-selective SAPO-34 zeolite membranes for enhanced conversion and selectivity in propane dehydrogenation membrane reactors. *Chem. Mater.* 28 (12), 4397–4402. <https://doi.org/10.1021/acs.chemmater.6b01458>.
- Kim, W., So, J., Choi, S., Liu, Y., Dixit, R.S., Sievers, C., et al., 2017. Hierarchical Ga-MFI catalysts for propane dehydrogenation. *Chem. Mater.* 29 (17), 7213–7222. <https://doi.org/10.1021/acs.chemmater.7b01566>.
- Kong, N., Fan, X., Liu, F., Wang, L., Lin, H., Li, Y., et al., 2020. Single vanadium atoms anchored on graphitic carbon nitride as a high-performance catalyst for non-oxidative propane dehydrogenation. *ACS Nano* 14 (5), 5772–5779. <https://doi.org/10.1021/acscatal.9b02459>.
- Kwak, J.H., Hu, J., Mei, D., Yi, C.W., Kim, D.H., Peden, C.H., et al., 2009. Coordinatively unsaturated Al³⁺ centers as binding sites for active catalyst phases of platinum on gamma-Al₂O₃. *Science* 325 (5948), 1670–1673. <https://doi.org/10.1126/science.1176745>.
- Langeslay, R.R., Kaphan, D.M., Marshall, C.L., Stair, P.C., Sattelberger, A.P., Delferro, M., 2018. Catalytic applications of vanadium: a mechanistic perspective. *Chem. Rev.* 119 (4), 2128–2191. <https://doi.org/10.1021/acs.chemrev.8b00245>.
- Larsson, M., Hultén, M., Blekkan, E.A., Andersson, B., 1996. The effect of reaction conditions and time on stream on the coke formed during propane dehydrogenation. *J. Catal.* 164 (1), 44–53. <https://doi.org/10.1006/jcat.1996.0361>.
- Li, P., Lang, W., Xia, K., Luan, L., Yan, X., Guo, Y., 2016. The promotion effects of Ni on the properties of Cr/Al catalysts for propane dehydrogenation reaction. *Appl. Catal. Gen.* 522, 172–179. <https://doi.org/10.1016/j.apcata.2016.05.007>.
- Li, B., Xu, Z., Chu, W., Luo, S., Jing, F., 2017. Ordered mesoporous Sn-SBA-15 as support for Pt catalyst with enhanced performance in propane dehydrogenation. *Chin. J. Catal.* 38 (4), 726–735. [https://doi.org/10.1016/S1872-2067\(17\)62805-5](https://doi.org/10.1016/S1872-2067(17)62805-5) (In Chinese).
- Li, J., Li, J., Zhao, Z., Fan, X., Liu, J., Wei, Y., et al., 2017. Size effect of TS-1 supports on the catalytic performance of PtSn/TS-1 catalysts for propane dehydrogenation. *J. Catal.* 352, 361–370. <https://doi.org/10.1016/j.jcat.2017.05.024>.
- Li, C., Guo, X., Shang, Q., Yan, X., Ren, C., Lang, W., et al., 2020. Defective TiO₂ for propane dehydrogenation. *Ind. Eng. Chem. Res.* 59 (10), 4377–4387. <https://doi.org/10.1021/acs.iecr.9b06759>.
- Lian, Z., Ali, S., Liu, T., Si, C., Li, B., Su, D.S., 2018. Revealing the janus character of the coke precursor in the propane direct dehydrogenation on Pt catalysts from a kMC simulation. *ACS Catal.* 8 (5), 4694–4704. <https://doi.org/10.1021/acscatal.8b00107>.
- Lillehaug, S., Børve, K.J., Sierka, M., Sauer, J., 2004. Catalytic dehydrogenation of ethane over mononuclear Cr (III) surface sites on silica. part I. Cr sites on α -bond metathesis. *J. Phys. Org. Chem.* 17 (11), 990–1006. <https://doi.org/10.1039/b303506a>.
- Liu, L., Corma, A., 2018. Metal catalysts for heterogeneous catalysis: from single atoms to nanoclusters and nanoparticles. *Chem. Rev.* 118, 4981–5079. <https://doi.org/10.1021/acs.chemrev.7b00776>.
- Liu, J., Liu, C., Ma, A., Rong, J., Da, Z., Zheng, A., Qin, L., 2016. Effects of Al₂O₃ phase and Cl component on dehydrogenation of propane. *Appl. Surf. Sci.* 368, 233–240. <https://doi.org/10.1016/j.apsusc.2016.01.282>.
- Liu, G., Zhao, Z., Wu, T., Zeng, L., Gong, J., 2016. Nature of the active sites of VO_x/Al₂O₃ catalysts for propane dehydrogenation. *ACS Catal.* 6 (8), 5207–5214. <https://doi.org/10.1021/acscatal.6b00893>.
- Liu, G., Zeng, L., Zhao, Z., Tian, H., Wu, T., Gong, J., 2016. Platinum-modified ZnO/Al₂O₃ for propane dehydrogenation: minimized platinum usage and improved catalytic stability. *ACS Catal.* 6 (4), 2158–2162. <https://doi.org/10.1021/acscatal.5b02878>.
- Liu, J., Yue, Y., Liu, H., Da, Z., Liu, C., Ma, A., et al., 2017. Origin of the robust catalytic performance of nanodiamond–graphene-supported Pt nanoparticles used in the propane dehydrogenation reaction. *ACS Catal.* 7 (5), 3349–3355. <https://doi.org/10.1021/acscatal.6b03452>.
- Liu, L., Meira, D.M., Arenal, R., Concepcion, P., Puga, A.V., Corma, A., 2019. Determination of the evolution of heterogeneous single metal atoms and nanoclusters under reaction conditions: which are the working catalytic sites? *ACS Catal.* 9 (12), 10626–10639. <https://doi.org/10.1021/acscatal.9b04214>.
- Liu, L., Lopez-Haro, M., Lopes, C.W., Rojas-Buzo, S., Concepcion, P., Manzanero, R., et al., 2020. Structural modulation and direct measurement of subnanometric bimetallic PtSn clusters confined in zeolites. *Nature Catalysis* 3 (8), 628–638. <https://doi.org/10.1038/s41929-020-0472-7>.
- Liu, D., He, Q., Ding, S., Song, L., 2020. Structural regulation and support coupling effect of single-atom catalysts for heterogeneous catalysis. *Advanced Energy Material* 10 (32), 2001482. <https://doi.org/10.1016/10.1002/aenm.202001482>.
- Liu, J., Liu, Y., Ni, Y., Liu, H., Zhu, W., Liu, Z., 2020. Enhanced propane dehydrogenation to propylene over zinc-promoted chromium catalysts. *Catalysis Science*

- & Technology 1 (6), 1739–1746. <https://doi.org/10.1039/c9cy01921a>.
- Liu, Q., Luo, M., Zhao, Z., Zhao, Q., 2020. K-modified Sn-containing dendritic mesoporous silica nanoparticles with tunable size and SnO_x-silica interaction for the dehydrogenation of propane to propylene. *Chem. Eng. J.* 380, 122423. <https://doi.org/10.1016/j.cej.2019.122423>.
- Long, L., Lang, W., Yan, X., Xia, K., Guo, Y., 2016. Yttrium-modified alumina as support for trimetallic PtSnIn catalysts with improved catalytic performance in propane dehydrogenation. *Fuel Process. Technol.* 146, 48–55. <https://doi.org/10.1016/j.fuproc.2016.02.012>.
- Ma, R., Yang, T., Gao, J., Kou, J., Zhu Chen, J., He, Y., et al., 2020. Composition tuning of Ru-based phosphide for enhanced propane selective dehydrogenation. *ACS Catal.* 10 (17), 10243–10252. <https://doi.org/10.1021/acscatal.0c01667.s001>.
- Mansoor, E., Head-Gordon, M., Bell, A.T., 2018. Computational modeling of the nature and role of Ga species for light alkane dehydrogenation catalyzed by Ga/H-MFI. *ACS Catal.* 8 (7), 6146–6162. <https://doi.org/10.1021/acscatal.7b04295>.
- Nakaya, Y., Hirayama, J., Yamazoe, S., Shimizu, K., Furukawa, S., 2020. Single-atom Pt in intermetallics as an ultrastable and selective catalyst for propane dehydrogenation. *Natural Communication* 11 (1). <https://doi.org/10.1038/s41467-020-16693-9>.
- Natarajan, P., Khan, H.A., Jaleel, A., Park, D.S., Kang, D., Yoon, S., et al., 2020. The pronounced effect of Sn on RhSn catalysts for propane dehydrogenation. *J. Catal.* 392, 8–20. <https://doi.org/10.1016/j.jcat.2020.09.016>.
- Nawaz, Z., 2015. Light alkane dehydrogenation to light olefin technologies: a comprehensive review. *Rev. Chem. Eng.* 31 (5). <https://doi.org/10.1515/energy.0078.000040>.
- Nykänen, L., Honkala, K., 2011. Density functional theory study on propane and propene adsorption on Pt (111) and PtSn alloy surfaces. *J. Phys. Chem. C* 115, 9578–9586. <https://doi.org/10.1021/jp1121799>.
- Nykänen, L., Honkala, K., 2013. Selectivity in propene dehydrogenation on Pt and Pt₃Sn surfaces from first principles. *ACS Catal.* 3 (12), 3026–3030. <https://doi.org/10.1021/cs400566y>.
- Olsbye, U., Virnøvskaia, A., Prytz, Ø., Tinnemans, S.J., Weckhuysen, B.M., 2005. Mechanistic insight in the ethane dehydrogenation reaction over Cr/Al₂O₃ catalysts. *Catal. Lett.* 103 (1–2), 143–148. <https://doi.org/10.1007/s10562-005-6521-7>.
- Otroshchenko, T., Sokolov, S., Stoyanova, M., Kondratenko, V.A., Rodemerck, U., Linke, D., et al., 2015. ZrO₂-Based alternatives to conventional propane dehydrogenation catalysts: active sites, design, and performance. *Angew. Chem. Int. Ed.* 54 (52), 15880–15883. <https://doi.org/10.1002/anie.201508731>.
- Otroshchenko, T.P., Rodemerck, U., Linke, D., Kondratenko, E.V., 2017. Synergy effect between Zr and Cr active sites in binary CrZrO_x or supported CrO_x/LaZrO_x: consequences for catalyst activity, selectivity and durability in non-oxidative propane dehydrogenation. *J. Catal.* 356, 197–205. <https://doi.org/10.1016/j.jcat.2017.10.012>.
- Otroshchenko, T.P., Vita, A.K., Uwe, R., David, L., Evgenii, V.K., 2017. Non-oxidative dehydrogenation of propane, n-butane, and isobutane over bulk ZrO₂-based catalysts: effect of dopant on the active site and pathways of product formation. *Catal. Sci. Technol.* 7, 4499–4510. <https://doi.org/10.1039/c7cy01583f>. In press.
- Peng, Z., Somodi, F., Helveg, S., Kisielowski, C., Specht, P., Bell, A.T., 2012. High-resolution in situ and ex-situ TEM studies on graphene formation and growth on Pt nanoparticles. *J. Catal.* 286, 22–29. <https://doi.org/10.1016/j.jcat.2011.10.008>.
- Pham, H.N., Sattler, J.J.H.B., Weckhuysen, B.M., Dartye, A.K., 2016. Role of Sn in the regeneration of Pt/γ-Al₂O₃ light alkane dehydrogenation catalysts. *ACS Catal.* 6, 2257–2264. <https://doi.org/10.1021/acscatal.5b02917.s001>.
- Purdy, S.C., Seemakurthi, R.R., Mitchell, G.M., Davidson, M., Lauderback, B.A., Deshpande, S., et al., 2020a. Structural trends in the dehydrogenation selectivity of palladium alloys. *Chem. Sci.* 11 (19), 5066–5081. <https://doi.org/10.1039/d0sc00875c>.
- Purdy, S.C., Ghanekar, P., Mitchell, G., Kropf, A.J., Zemlyanov, D.Y., Ren, Y., et al., 2020b. Origin of electronic modification of platinum in a Pt₃V alloy and its consequences for propane dehydrogenation catalysis. *ACS Appl. Energy Mater.* 3 (2), 1410–1422. <https://doi.org/10.1016/j.jcat.2018.08.001>.
- Puurunen, R.L., Beheydt, B.G., Weckhuysen, B.M., 2001. Monitoring chromia/alumina catalysts in situ during propane dehydrogenation by optical fiber UV–visible diffuse reflectance spectroscopy. *Journal of Catalysts* 204 (1), 253–257. <https://doi.org/10.1006/jcat.2001.3372>.
- Raman, N., Maisel, S., Grabau, M., Taccardi, N., Debuschewitz, J., Wolf, M., et al., 2019. Highly effective propane dehydrogenation using Ga–Rh supported catalytically active liquid metal solutions. *ACS Catal.* 9 (10), 9499–9507. <https://doi.org/10.1021/acscatal.9b02459>.
- Redekop, E.A., Saerens, S., Galvita, V.V., et al., 2016a. Early stages in the formation and burning of graphene on a Pt(Mg/Al)O dehydrogenation catalyst: a temperature- and time-resolved study. *J. Catal.* 344, 482–495. <https://doi.org/10.1016/j.jcat.2016.10.023>.
- Redekop, E.A., Saerens, S., Galvita, V.V., Gonz, C., Specht, P., Bell, A.T., 2016b. High-resolution in situ and ex-situ TEM stuanid burning of graphene on a Pt(Mg/Al)O dehydrogenation catalyst: a temperature- and time-resolved study. *J. Catal.* 344, 482–495. <https://doi.org/10.1016/j.jcat.2016.10.023>.
- Ren, G., Pei, G., Ren, Y., Liu, K., Chen, Z., Yang, J., et al., 2018. Effect of group IB metals on the dehydrogenation of propane to propylene over anti-sintering Pt/MgAl₂O₄. *J. Catal.* 366, 115–126. <https://doi.org/10.1016/j.jcat.2018.08.001>.
- Rochlitz, L., Searles, K., Alfke, J., Zemlyanov, D., Safonova, O.V., Copéret, C., 2020. Silica-supported, narrowly distributed, subnanometric Pt–Zn particles from single sites with high propane dehydrogenation performance. *Chem. Sci.* 11 (6), 1549–1555. <https://doi.org/10.1039/C9SC05599A>.
- Rodemerck, U., Stoyanova, M., Kondratenko, E.V., Linke, D., 2017. Influence of the kind of VO_x structures in VO_x/MCM-41 on activity, selectivity and stability in dehydrogenation of propane and isobutane. *J. Catal.* 352, 256–263. <https://doi.org/10.1016/j.jcat.2017.05.022>.
- Rossi, S.D., Ferraris, G., Fremiotti, S., Cimino, A., Indovina, V., 1992. Propane dehydrogenation on chromia/zirconia catalysts. *Appl. Catal. Gen.* 81 (1), 113–132. [https://doi.org/10.1016/0926-860X\(92\)80264-D](https://doi.org/10.1016/0926-860X(92)80264-D).
- Ruiz Puigdollers, A., Schlexer, P., Tosoni, S., Pacchioni, G., 2017. Increasing oxide reducibility: the role of metal/oxide interfaces in the formation of oxygen vacancies. *ACS Catal.* 7 (10), 6493–6513. <https://pubs.acs.org/doi/10.1021/acscatal.7b01913>.
- Ryoo, R., Kim, J., Jo, C., Han, S.W., Kim, J., Park, H., et al., 2020. Rare-earth–platinum alloy nanoparticles in mesoporous zeolite for catalysis. *Nature* 585 (7824), 221–224. <https://doi.org/10.1038/s41586-020-2671-4>.
- Saelee, T., Namuangruk, S., Kungwan, N., Junkaew, A., 2018. Theoretical insight into catalytic propane dehydrogenation on Ni (111). *J. Phys. Chem. C* 122 (26), 14678–14690. <https://doi.org/10.1021/acs.jpcc.8b03939.s001>.
- Saerens, S., Sabbe, M.K., Galvita, V.V., Redekop, E.A., Reyniers, M., Marin, G.B., 2017. The positive role of hydrogen on the dehydrogenation of propane on Pt (111). *ACS Catal.* 7 (11), 7495–7508. <https://doi.org/10.1021/acscatal.7b01584>.
- Santhoshkumar, M., Hammer, N., Ronning, M., Holmen, A., Chen, D., Walmsley, J., et al., 2009. The nature of active chromium species in Cr-catalysts for dehydrogenation of propane: new insights by a comprehensive spectroscopic study. *Journal of Catalysts* 261 (1), 116–128. <https://doi.org/10.1016/j.jcat.2008.11.014>.
- Sattler, J.J.H.B., Beale, A.M., Weckhuysen, B.M., 2013. Operando Raman spectroscopy study on the deactivation of Pt/Al₂O₃ and Pt-Sn/Al₂O₃ propane dehydrogenation catalysts. *Phys. Chem. Chem. Phys.* 15 (29). <https://doi.org/10.1039/c3cp50646k>.
- Sattler, J.J.H.B., Ruiz-Martinez, J., Santillan-Jimenez, E., Weckhuysen, B.M., 2014a. Catalytic dehydrogenation of light alkanes on metals and metal oxides. *Chem. Rev.* 114 (20), 10613–10653. <https://doi.org/10.1021/cr50024362>.
- Sattler, J.J.H.B., Gonzalez-Jimenez, I.D., Luo, L., Stears, B.A., Malek, A., Barton, D.G., et al., 2014b. Platinum-promoted Ga/Al₂O₃ as highly active, selective, and stable catalyst for the dehydrogenation of propane. *Angew. Chem. Int. Ed.* 53 (35), 9251–9256. <https://doi.org/10.1002/anie.201404460>.
- Schreiber, M.W., Plaisance, C.P., Baumgärtel, M., Reuter, K., Jentys, A., Bermejo-Deval, R., et al., 2018. Lewis–brønsted acid pairs in Ga/H-ZSM-5 to catalyze dehydrogenation of light alkanes. *J. Am. Chem. Soc.* 140 (14), 4849–4859. <https://doi.org/10.1021/jacs.7b12901>.
- Schweitzer, N.M., Hu, B., Das, U., Kim, H., Greeley, J., Curtiss, L.A., et al., 2014a. Propylene hydrogenation and propane dehydrogenation by a single-site Zn²⁺ on silica catalyst. *ACS Catal.* 4 (4), 1091–1098. <https://doi.org/10.1021/cs401116p>.
- Schweitzer, N.M., Hu, B., Das, U., Kim, H., Greeley, J., Curtiss, L.A., et al., 2014b. Propylene hydrogenation and propane dehydrogenation by a single-site Zn²⁺ on silica catalyst. *ACS Catal.* 4 (4), 1091–1098. <https://pubs.acs.org/doi/10.1021/cs401116p>.
- Searles, K., Chan, K.W., Mendes Burak, J.A., Zemlyanov, D., Safonova, O., Copéret, C., 2018. Highly productive propane dehydrogenation catalyst using silica-supported Ga–Pt nanoparticles generated from single-sites. *J. Am. Chem. Soc.* 140 (37), 11674–11679. <https://doi.org/10.1021/jacs.8b05378>.
- Shan, Y., Sui, Z., Zhu, Y., Chen, D., Zhou, X., 2015. Effect of steam addition on the structure and activity of Pt–Sn catalysts in propane dehydrogenation. *Chem. Eng. J.* 278, 240–248. <https://doi.org/10.1016/j.cej.2014.09.107>.
- Shi, L., Deng, G., Li, W., Miao, S., Wang, Q., Zhang, W., et al., 2015. Al₂O₃ nanosheets rich in pentacoordinate Al³⁺ ions stabilize Pt–Sn clusters for propane dehydrogenation. *Angew. Chem. Int. Ed.* 54 (47), 13994–13998. <https://doi.org/10.1002/ange.201507119>.
- Sokolov, S., Stoyanova, M., Rodemerck, U., Linke, D., Kondratenko, E.V., 2012. Comparative study of propane dehydrogenation over V-, Cr-, and Pt-based catalysts: time on-stream behavior and origins of deactivation. *J. Catal.* 293, 67–75. <https://doi.org/10.1016/j.jcat.2012.06.005>.
- Sun, Y., Tao, L., You, T., Li, C., Shan, H., 2014. Effect of sulfation on the performance of Fe₂O₃/Al₂O₃ catalyst in catalytic dehydrogenation of propane to propylene. *Chem. Eng. J.* 244, 145–151. <https://doi.org/10.1016/j.cej.2014.01.047>.
- Sun, Y., Wu, Y., Shan, H., Wang, G., Li, C., 2015. Studies on the promoting effect of sulfate species in catalytic dehydrogenation of propane over Fe₂O₃/Al₂O₃ catalysts. *Catalysis Science & Technology* 5 (2), 1290–1298. <https://doi.org/10.1039/C4CY01163E>.
- Sun, G., Zhao, Z., Mu, R., Zha, S., Li, L., Chen, S., et al., 2018. Breaking the scaling relationship via thermally stable Pt/Cu single atom alloys for catalytic dehydrogenation. *Nat. Commun.* 9 (1). <https://doi.org/10.1038/s41467-018-06967-8>.
- Sun, X., Han, P., Li, B., Zhao, Z., 2018. Tunable catalytic performance of single Pt atom on doped graphene in direct dehydrogenation of propane by rational doping: a density functional theory study. *J. Phys. Chem. C* 122 (3), 1570–1576. <https://doi.org/10.1021/acs.jpcc.7b09736>.
- Szeto, K.C., Jones, Z.R., Merle, N., Rios, C., Gallo, A., Le Quemener, F., et al., 2018. A strong support effect in selective propane dehydrogenation catalyzed by Ga(i-Bu)₃ grafted onto γ-alumina and silica. *ACS Catal.* 8 (8), 7566–7577. <https://doi.org/10.1021/acscatal.8b00936>.
- Tan, S., Hu, B., Kim, W., Pang, S.H., Moore, J.S., Liu, Y., et al., 2016. Propane dehydrogenation over alumina-supported iron/phosphorus catalysts: structural evolution of iron species leading to high activity and propylene selectivity. *ACS*

- Catal. 6 (9), 5673–5683. <https://doi.org/10.1021/acscatal.6b01286>.
- Uemura, Y., Inada, Y., Bando, K.K., Sasaki, T., Kamiuchi, N., Eguchi, K., et al., 2011. Core–Shell phase separation and structural transformation of Pt₃Sn alloy nanoparticles supported on γ -Al₂O₃ in the reduction and oxidation processes characterized by in situ time-resolved XAFS. *J. Phys. Chem. C* 115 (13), 5823–5833. <https://doi.org/10.1021/jp111286b>.
- Valcárcel, A., Ricart, J.M., Clotet, A., Markovits, A., Minot, C., Illas, F., 2002. Theoretical study of the structure of propene adsorbed on Pt (111). *Surf. Sci.* 519 (3), 250–258. [https://doi.org/10.1016/S0039-6028\(02\)02220-3](https://doi.org/10.1016/S0039-6028(02)02220-3).
- Virnovskaia, A., Morandi, S., Rytter, E., Ghiotti, G., Olsbye, U., 2007. Characterization of PtSn/Mg(Al)O catalysts for light alkane dehydrogenation by FT-IR spectroscopy and catalytic measurements. *J. Phys. Chem. C* 111 (40), 14732–14742. <https://doi.org/10.1021/jp074686u>.
- Vu, B.K., Song, M.B., Ahn, I.Y., Suh, Y., Suh, D.J., Kim, W., et al., 2016. Propane dehydrogenation over Pt–Sn/Rare-earth-doped Al₂O₃: influence of La, Ce, or Y on the formation and stability of Pt–Sn alloys. *Catal. Today* 164 (1), 214–220. <https://doi.org/10.1016/j.cattod.2010.10.007>.
- Waku, T., Biscardi, J.A., Iglesia, E., 2003. Active, selective, and stable Pt/Na–[Fe]ZSM-5 catalyst for the dehydrogenation of light alkanes. *Chem. Commun.* (14), 1764. <https://doi.org/10.1039/b303506a>.
- Wang, G., Zhang, H., Wang, H., Zhu, Q., Li, C., Shan, H., 2016. The role of metallic Sn species in catalytic dehydrogenation of propane: active component rather than only promoter. *J. Catal.* 344, 606–608. <https://doi.org/10.1016/j.jcat.2017.04.018>.
- Wang, H., Sun, L., Sui, Z., Zhu, Y., Ye, G., Chen, D., et al., 2018. coke formation on Pt–Sn/Al₂O₃ catalyst for propane dehydrogenation. *Ind. Eng. Chem. Res.* 57 (26), 8647–8654. <https://doi.org/10.1021/acs.iecr.8b01313>.
- Wang, Y., Hu, Z., Tian, W., Gao, L., Wang, Z., Yuan, Z., 2019. Framework-confined Sn in Si-beta stabilizing ultra-small Pt nanoclusters as direct propane dehydrogenation catalysts with high selectivity and stability. *Catalysis science & technology* 9 (24), 6993–7002. <https://doi.org/10.1039/c9cy01907c>.
- Wang, Y., Hu, Z., Lv, X., Chen, L., Yuan, Z., 2020. Ultrasmall PtZn bimetallic nanoclusters encapsulated in silicalite-1 zeolite with superior performance for propane dehydrogenation. *J. Catal.* 385, 61–69. <https://doi.org/10.1016/j.jcat.2020.02.019>.
- Wang, G., Zhu, X., Li, C., 2020. Recent progress in commercial and novel catalysts for catalytic dehydrogenation of light alkanes. *Chem. Rec.* 20 (6), 604–616. <https://doi.org/10.1002/tcr.201900090c>.
- Wang, H., Huang, H., Bashir, K., Li, C., 2020. Isolated Sn on mesoporous silica as a highly stable and selective catalyst for the propane dehydrogenation. *Appl. Catal. Gen.* 590, 117291. <https://doi.org/10.1016/j.apcata.2019.117291>.
- Wang, P., Xu, Z., Wang, T., Yue, Y., Bao, X., Zhu, H., 2020. Unmodified bulk alumina as an efficient catalyst for propane dehydrogenation. *Catalysis Science & Technology* 10 (11), 3537–3541. <https://doi.org/10.1039/D0CY00779j>.
- Wu, J., Helveg, S., Ullmann, S., Peng, Z., Bell, A.T., 2016. Growth of encapsulating carbon on supported Pt nanoparticles studied by in situ TEM. *J. Catal.* 338, 295–304. <https://doi.org/10.1016/j.jcat.2016.03.010>.
- Wu, T., Liu, G., Zeng, L., Sun, G., Chen, S., Mu, R., et al., 2017. Structure and catalytic consequence of Mg-modified VO_x/Al₂O₃ catalysts for propane dehydrogenation. *AIChE J.* 63 (11), 4911–4919. <https://doi.org/10.1002/aic.15836>.
- Wu, Z., Bukowski, B.C., Li, Z., Milligan, C., Zhou, L., Ma, T., et al., 2018. Changes in catalytic and adsorptive properties of 2 nm Pt₃Mn nanoparticles by subsurface atoms. *J. Am. Chem. Soc.* 140 (44), 14870–14877. <https://doi.org/10.1021/jacs.8b08162.s001>.
- Xia, K., Lang, W., Li, P., Yan, X., Guo, Y., 2016. The properties and catalytic performance of PtIn/Mg(Al)O catalysts for the propane dehydrogenation reaction: effects of pH value in preparing Mg(Al)O supports by the co-precipitation method. *J. Catal.* 338, 104–114. <https://doi.org/10.1016/j.jcat.2016.02.028>.
- Xie, Z., Ren, Y., Li, J., Zhao, Z., Fan, X., Liu, B., et al., 2019. Facile in situ synthesis of highly dispersed chromium oxide incorporated into mesoporous ZrO₂ for the dehydrogenation of propane with CO₂. *J. Catal.* 372, 206–216. <https://doi.org/10.1016/j.jcat.2019.02.026>.
- Xie, Y., Luo, R., Sun, G., Chen, S., Zhao, Z., Mu, R., et al., 2020. Facilitating the reduction of V–O bonds on VO_x/ZrO₂ catalysts for non-oxidative propane dehydrogenation. *Chem. Sci.* 11 (15), 3845–3851. <https://doi.org/10.1039/D0SC00690D>.
- Xiong, H., Lin, S., Goetze, J., Pletcher, P., Guo, H., Kovarik, L., et al., 2017. Thermally stable and regenerable platinum-tin clusters for propane dehydrogenation prepared by atom trapping on ceria. *Angew. Chem.* 129 (31), 9114–9119. <https://doi.org/10.1016/10.1002/ange.201701115>.
- Xu, Y., Chen, J., Yuan, X., Zhang, Y., Yu, J., Liu, H., et al., 2018. Sintering-resistant Pt on Ga₂O₃ rods for propane dehydrogenation: the morphology matters. *Ind. Eng. Chem. Res.* 57 (39), 13087–13093. <https://doi.org/10.1021/acs.iecr.8b03085>.
- Xu, Z., Yue, Y., Bao, X., Xie, Z., Zhu, H., 2019a. Propane dehydrogenation over Pt clusters localized at the Sn single-site in zeolite framework. *ACS Catal.* 10 (1), 818–828. <https://doi.org/10.1016/10.1021/acscatal.9b03527>.
- Xu, Z., Xu, R., Yue, Y., Yuan, P., Bao, X., Abou-Hamad, E., et al., 2019b. Bimetallic Pt–Sn nanocluster from the hydrogenolysis of a well-defined surface compound consisting of [(≡AlO)Pt(COD)Me] and [(≡AlO)SnPh₃] fragments for propane dehydrogenation. *J. Catal.* 374, 391–400. <https://doi.org/10.1016/j.jcat.2019.04.035>.
- Yang, M., Zhu, Y., Fan, C., Sui, Z., Chen, D., Zhou, X., 2010. Density functional study of the chemisorption of C1, C2 and C3 intermediates in propane dissociation on Pt (111). *J. Mol. Catal. Chem.* 321 (1–2), 42–49. <https://doi.org/10.1016/j.molcata.2010.01.017>.
- Yang, M., Zhu, Y., Fan, C., Sui, Z., Chen, D., Zhou, X., 2011. DFT study of propane dehydrogenation on Pt catalyst: effects of step sites. *Phys. Chem. Chem. Phys.* 13 (8), 3257. <https://doi.org/10.1039/c0cp00341g>.
- Yang, M., Zhu, Y., Zhou, X., Sui, Z., Chen, D., 2012. First-principles calculations of propane dehydrogenation over PtSn catalysts. *ACS Catal.* 2 (6), 1247–1258. <https://doi.org/10.1021/acs.cemmater.6b01458.s001>.
- Ye, G., Wang, H., Duan, X., Sui, Z., Zhou, X., Coppens, M., et al., 2019. Pore network modeling of catalyst deactivation by coking, from single site to particle, during propane dehydrogenation. *AIChE J.* 65 (1), 140–150. <https://doi.org/10.1002/aic.16410>.
- Ye, C., Mao, P., Wang, Y., Zhang, N., Wang, D., Jiao, M., et al., 2020. Surface hexagonal Pt₁Sn₁ intermetallic on Pt nanoparticles for selective propane dehydrogenation. *ACS Appl. Mater. Interfaces* 12 (23), 25903–25909. <https://doi.org/10.1021/acsmi.0c05043>.
- Yu, Q., Yu, T., Chen, H., Fang, G., Pan, X., Bao, X., 2020. The effect of Al³⁺ coordination structure on the propane dehydrogenation activity of Pt/Ga/Al₂O₃ catalysts. *Journal of Energy Chemistry* 41, 93–99 (In Chinese), CNKI:SUN:TRQZ.0.2020-02-014.
- Zangeneh, F.T., Taeb, A., Gholivand, K., Sahebdehfar, S., 2015. The effect of mixed HCl_s localized at the Pt adsorption and catalytic properties of Pt–Sn/Al₂O₃ catalysts in propane dehydrogenation. *Appl. Surf. Sci.* 357, 172–178. <https://doi.org/10.1016/j.apsusc.2015.08.235>.
- Zhang, Y., Zhou, Y., Huang, L., Zhou, S., Sheng, X., Wang, Q., et al., 2015. Structure and catalytic properties of the Zn-modified ZSM-5 supported platinum catalyst for propane dehydrogenation. *Chem. Eng. J.* 270, 352–361. <https://doi.org/10.1016/j.cej.2015.01.008>.
- Zhang, Y., Zhao, Y., Otroshchenko, T., Lund, H., Pohl, M., Rodemerck, U., et al., 2018. Control of coordinatively unsaturated Zr sites in ZrO₂ for efficient C–H bond activation. *Nat. Commun.* 9 (1), 1–10. <https://doi.org/10.1038/s41467-018-06174-5>.
- Zhang, Y., Yang, S., Lu, J., Mei, Y., He, D., Luo, Y., 2019a. Effect of a Ce promoter on nonoxidative dehydrogenation of propane over the commercial Cr/Al₂O₃ catalyst. *Ind. Eng. Chem. Res.* 58 (43), 19818–19824. <https://doi.org/10.1021/acs.iecr.9b03870>.
- Zhang, Y., Zhao, Y., Otroshchenko, T., Han, S., Lund, H., Rodemerck, U., et al., 2019b. The effect of phase composition and crystallite size on activity and selectivity of ZrO₂ in non-oxidative propane dehydrogenation. *J. Catal.* 371, 313–324. <https://doi.org/10.1016/j.jcat.2019.02.012>.
- Zhang, Y., Zhao, Y., Otroshchenko, T., Perechodjuk, A., Kondratenko, V.A., Bartling, S., et al., 2020. Structure–activity–selectivity relationships in propane dehydrogenation over Rh/ZrO₂ catalysts. *ACS Catal.* 10 (11), 6377–6388. <https://doi.org/10.1021/10.1021/acscatal.0c01455>.
- Zhao, Z.J., Chiu, C.C., Gong, J., 2015. Molecular understandings on the activation of light hydrocarbons over heterogeneous catalysts. *Chem. Sci.* 6 (8), 4403–4425. <https://doi.org/10.1039/c5sc01227a>.
- Zhao, Z., Wu, T., Xiong, C., Sun, G., Mu, R., Zeng, L., et al., 2018. Hydroxyl-mediated non-oxidative propane dehydrogenation over VO_x/γ-Al₂O₃ catalysts with improved stability. *Angew. Chem. Int. Ed.* 57 (23), 6791–6795. <https://doi.org/10.1002/anie.201800123>.
- Zhao, D., Li, Y., Han, S., Zhang, Y., Jiang, G., Wang, Y., et al., 2019. ZnO nanoparticles encapsulated in nitrogen-doped carbon material and silicalite-1 composites for efficient propane dehydrogenation. *iScience* 13, 269–276. <https://doi.org/10.1016/j.isci.2019.02.018>.
- Zheng, B., Hua, W., Yue, Y., Gao, Z., 2005. Dehydrogenation of propane to propene over different polymorphs of gallium oxide. *J. Catal.* 232 (1), 143–151. <https://doi.org/10.1016/j.jcat.2005.03.001>.
- Zhu, H., Anjum, D.H., Wang, Q., Abou-Hamad, E., Emsley, L., Dong, H., et al., 2014. Sn surface-enriched Pt/graphene in Direct Dehydrogenation selective and stable catalyst for propane dehydrogenation. *Journal of Catalysts* 320, 52–62. <https://doi.org/10.1016/j.jcat.2014.09.013>.
- Zhu, J., Yang, M., Yu, Y., Zhu, Y., Sui, Z., Zhou, X., et al., 2015. Size-dependent reaction mechanism and kinetics for propane dehydrogenation over Pt catalysts. *ACS Catal.* 5 (11), 6310–6319. <https://doi.org/10.1021/acscatal.5b01423>.
- Zhu, Y., An, Z., Song, H., Xiang, X., Yan, W., He, J., 2017. Lattice-confined Sn_(IV) stabilizing raft-like Pt clusters: high selectivity and durability in propane dehydrogenation. *ACS Catal.* 7 (10), 6973–6978. <https://doi.org/10.1021/acscatal.7b02264>.